On spectral statistics of classically integrable systems

1998 J. Phys. A: Math. Gen. 31 4669

(http://iopscience.iop.org/0305-4470/31/20/008)

J. Phys. A: Math. Gen. **31** (1998) 4669–4704. Printed in the UK PII: S0305-4470(98)90628-X

On spectral statistics of classically integrable systems

Marko Robnik† and Gregor Veble‡

Center for Applied Mathematics and Theoretical Physics, University of Maribor, Krekova 2, SLO-2000 Maribor, Slovenia

Received 12 January 1998, in final form 3 March 1998

Abstract. This work is an extensive study of the spectral statistics of three representative classically integrable systems, namely rectangle, torus and circle billiards. We analyse the $E(k, L)$ statistics and focus on the related level spacing distribution $P(S)$ and the delta statistics $\Delta(L)$. The agreement with the Poissonian model is *typically* found to be perfect up to the outer (unfolded) energy scale $L < L_{\max}$, beyond which the saturation is observed, in agreement with Berry's dynamical theory of the spectral rigidity, where $L_{\max} \to \infty$ as $\bar{h} \to 0$.

The *untypical* systems are those, where for example $P(S)$ is not a smooth distribution but a sum of the delta functions, due to the 'granularity' of the energy scale, for example in the rectangle with the rational squared sides ratio. However, even there we find reasonable trend towards Poissonian statistics for large ranges L but $L \leqslant L_{\max}$. We describe theoretically and numerically the broadening of the delta spikes when the rectangular billiard is slightly distorted away from a rational to an irrational shape and find excellent agreement. Also, in irrational rectangle billiards we show and explain the existence of large fluctuations, by one order of magnitude bigger than the statistical ones, whose origin is in the closeness to some rational billiard shape. These fluctuations and their amplitude are independent of the energy if the bin size shrinks inversely with energy.

Finally we tested the mode distribution (i.e. distribution of the reduced mode fluctuation number W) and found that it was not Poissonian, in agreement with Steiner's conjecture, and in fact follows the prediction by Bleher *et al*, that its tail behaves as $\exp(-W^4)$. The general reason for non-universal behaviour of $P(W)$ is that at largest energy scales we are always in the saturation regime $L \geqslant L_{\max}$.

1. Introduction

The spectral statistics of classically integrable systems has been assumed to obey the Poissonian laws at all ranges L of the unfolded spectrum in the strict semiclassical limit when the Planck constant goes to zero, $\bar{h} \to 0$, and we collect asymptotically infinitely many levels in a given (narrow) energy interval, within which the classical dynamics is sharply defined and has the same phase portrait at all energies inside. The class of integrable systems thus constitutes the Poissonian universality class of spectral fluctuations, to be distinguished from the GOE and GUE ensembles of random matrices, which—according to the Bohigas conjecture (Bohigas *et al* 1984)—correctly describe the spectral statistics of the fully chaotic systems (ergodic or more chaotic), depending on whether they have a time reversal symmetry (GOE), or not (GUE) (or any other antiunitary symmetry (Berry and Robnik 1986, Robnik and Berry 1986, Robnik 1986), for some modifications see also Leyvraz *et al* (1996) and Keating and Robbins (1997)). After the early contributions towards a proof of the Bohigas

† E-mail address: robnik@uni-mb.si
‡ E-mail address: gregor.veble@uni-mb.si

0305-4470/98/204669+36$19.50

conjecture by Berry (1985) there was more than a decade of theoretical silence, broken recently by a paper by Andreev *et al* (1996), which is still conjectural but has the potential of a rigorous proof. Further work along these lines is in progress (Keating and Bogomolny 1996, Weidenmüller 1997).

For an excellent review of quantum chaos see the recent paper by Weidenmüller *et al* (Guhr *et al* 1997).

In view of the integrable (Poissonian) universality class we have the early work by Berry and Tabor (1977), based on the torus quantization approximation, i.e. the EBK or WKB approximation. However, since EBK is only an approximation, their result is a rather lucky circumstance, because Poissonian statistics has no level repulsion phenomenon. The level spacing distribution is $P(S) = \exp(-S)$, and thus $P(S \neq 0) \neq 0$. Namely, the phenomenon of the energy level repulsion cannot be captured by any semiclassical approximation at any order (Robnik 1986, Prosen and Robnik 1993, Robnik and Salasnich 1997a, b). Heuristically, Poissonian statistics is quite obvious if we have two or more degrees of freedom and therefore two or more integrals of motion and two or more quantum numbers. Essentially we superpose an infinite number of number sequences of equal statistical weight and thus the result ought to be Poissonian (Robnik 1986), except when the mean spacings are somehow rationally connected such that for example the limiting $P(S)$ does not exist, but is a sum of delta functions instead. This has been assumed to hold true for quite some time, with the intermediate period of some new discoveries (Casati *et al* 1985, Seligman and Verbaarschot 1986, Feingold 1985) and discussions, which brought some reservations. Later, it was shown by Shnirelman (1993), that quite generally in systems with time reversal symmetry one should observe the so-called Shnirelman peak, i.e. the delta function peak of $P(S)$ at $S = 0$. However this can usually be quite easily removed by considering and separating the symmetries of the system. What is left in an integrable system after such desymmetrization is a spectrum with the Poissonian statistics. Recently it was shown (Bleher *et al* 1993) that in some special integrable systems we find deviations from the Poissonian behaviour in the so-called mode distribution $P(W)$ (= the distribution of the reduced mode fluctuation number W). Steiner (1994) postulated that this distribution should behave non-Gaussian in integrable systems, and Gaussian in chaotic systems (GOE, GUE). We shall discuss this in detail and show how that is compatible with the Poissonian behaviour for example of the $E(k, L)$ statistics up to $L \leqslant L_{\max}$. The explanation is that on the largest energy ranges implicitly contained in the statistics of W we are always in the non-universal, dynamical saturation regime $L \geqslant L_{\max}$.

The non-universal but generic classes of behaviour (of systems with mixed classical dynamics such as, e.g. KAM-type systems) will not be discussed in this work, although they are in a sense the most important ones. They can be understood theoretically once the universality classes are understood (Berry and Robnik 1984, Prosen and Robnik 1993a, b, 1994a, b, Robnik 1997, Robnik and Prosen 1997).

The main message of this paper is that the Poissonian model is almost perfect for the classically integrable systems that we study here, although the untypical systems can of course deviate from that model, and their vicinity affects the approach to the high-energy Poissonian behaviour even in typical integrable systems such as irrational rectangle billiards.

The *untypical* systems are those, where for example $P(S)$ is not a smooth distribution but a sum of the delta functions instead, due to the 'granularity' of the energy scale, for example in the rectangle with the rational squared sides ratio. However, even there, we find a reasonable trend towards Poissonian statistics for large ranges L. We shall describe both theoretically and numerically what happens when the rectangle billiard is slightly distorted away from a rational to an irrational shape. The delta spikes broaden and we illustrate

numerically our excellent theoretical prediction of this broadening. Also, in irrational rectangle billiards we show and explain the existence of large fluctuations, by an order of magnitude bigger than the statistical (Poissonian) ones, whose origin is in the closeness to some rational billiard shape. These fluctuations and their amplitude are independent of the energy if the bin size shrinks reciprocally with the (unfolded) energy.

This paper is organized as follows. First we shall present some basic definitions, concepts and theoretical results, then we show the results and theory for the rectangle billiard, followed by the torus and the circle billiards, concluding with general results and discussions.

2. Some definitions and basic concepts

We shall assume that all our spectra are unfolded. This means that the sequence of the actual (physical) energy levels

$$\{E_1, E_2, \ldots, E_i, \ldots\} \tag{1}$$

is transformed to the sequence of numbers $\{x_i\}$ using the mean density of levels

$$\rho(E) = \frac{1}{(2\pi\hbar)^f} \int \delta(E - H(\boldsymbol{q}, \boldsymbol{p}))\, \mathrm{d}^f \boldsymbol{q}\, \mathrm{d}^f \boldsymbol{p} \tag{2}$$

where $\delta(E - H)$ is the Dirac delta function, f is the number of degrees of freedom, $\boldsymbol{q}, \boldsymbol{p}$ are the coordinates and momenta in the classical phase space and $H(\boldsymbol{q}, \boldsymbol{p})$ is the classical Hamilton function of the underlying Hamiltonian system whose quantal statistics shall be analysed. Equation (2) is nothing but the Thomas–Fermi rule. It is the leading term of the famous Weyl formula for billiard systems. Denoting the cumulative mean number of levels up to the energy E by

$$\overline{N}(E) = \int_{-\infty}^{E} \rho(z)\, \mathrm{d}z \tag{3}$$

we define *the unfolded energy* x_i as

$$x_i = \overline{N}(E_i). \tag{4}$$

Therefore the spectral staircase function after the unfolding procedure can be written as

$$N(x) = \sum_{i=1}^{\infty} \Theta(x - x_i) \tag{5}$$

where $\Theta(x)$ is the Heaviside unit step function. $N(x)$ can be split into the mean smooth part x and the fluctuating part $N_{\mathrm{fluc}}(x)$,

$$N(x) = x + N_{\mathrm{fluc}}(x) \tag{6}$$

where the construction of the unfolded spectrum $\{x_i\}$ now has a unit mean level spacing, whilst the average of $N_{\mathrm{fluc}}(x)$ over a suitable energy range of the same unfolded spectrum vanishes by definition. The two most important spectral measures will be considered, the level spacing distribution $P(S)$, and the Δ statistics defined in the standard way by

$$\Delta(L) = \left\langle \min_{A,B} \frac{1}{L} \int_{\alpha}^{\alpha+L} [N(x) - Ax - B]^2\, \mathrm{d}x \right\rangle_{\alpha}. \tag{7}$$

Sometimes it is useful to also know the number variance, denoted by $\Sigma^2(L)$, the dispersion of the number of levels $n(L)$ in an interval of length L, where $\langle n(L) \rangle = L$, and

$$\Sigma^2(L) = \langle (n(L) - L)^2 \rangle = L - 2 \int_0^L (L - r) Y_2(r)\, \mathrm{d}r \tag{8}$$

where $Y_2(r)$ is the pair cluster function (Bohigas 1991, Haake 1992, Mehta 1991). There also exists a connection between Σ^2 and Δ,

$$\Delta(L) = \frac{2}{L^4}\int_0^L (L^3 - 2L^2 r + r^3)\Sigma^2(r)\,\mathrm{d}r \tag{9}$$

although, strictly speaking, this has heretofore been proven only within the context of RMT (Aurich *et al* 1997, Mehta 1991). Finally, we shall consider not the set of all the cluster functions $Y_n(x_1, x_2, \ldots, x_n)$, where $n = 2, 3, \ldots$, but rather the so-called $E(k, L)$ statistics, for all $k = 0, 1, 2, \ldots$, following the suggestion of Steiner and co-workers (Aurich *et al* 1997), because they are very easy to calculate numerically and yet contain all information concerning spectral statistics. By definition $E(k, L)$ is *the probability* that inside an interval of length L we find exactly k levels. There are simple relationships to other statistical quantities. For example, the level spacing distribution $P(S)$ is

$$P(S) = \frac{\partial^2}{\partial L^2}E(k = 0, L = S) \tag{10}$$

and

$$\Sigma^2(L) = \sum_{k=0}^{\infty}(k - L)^2 E(k, L) \tag{11}$$

and therefore, through (9), we have the relation expressing $\Delta(L)$ in terms of the $E(k, L)$ statistics.

We now state the results for the Poissonian statistics. By definition the Poissonian statistics is such that if they are on the average L events, then the probability to actually observe k events is given by

$$E_{\mathrm{Poisson}}(k, L) = \frac{L^k}{k!}\exp(-L). \tag{12}$$

From this definition it is easily derived (see (10))

$$P_{\mathrm{Poisson}}(S) = \exp(-S) \tag{13}$$

and after (11)

$$\Sigma^2_{\mathrm{Poisson}}(L) = L \tag{14}$$

and then using (9)

$$\Delta_{\mathrm{Poisson}}(L) = \frac{L}{15}. \tag{15}$$

Poissonian statistics also means by definition that there are no correlations, i.e. the pair correlation function factorizes, so that for the pair cluster function we have (cf Mehta 1991, Bohigas 1991)

$$Y_2^{\mathrm{Poisson}}(x) = 0. \tag{16}$$

Thus, applying this fact to equation (8) and then (9) we again recover Poissonian values (14) and (15).

The most important and convenient objects to observe numerically, or experimentally, are the $E(k, L)$ statistics. They have a maximum near $L \approx k$ which is the range that we shall observe them most carefully.

Finally we define the mode distribution. By this we mean the distribution of *the reduced mode number* $W(x)$, defined by

$$W(x) = \frac{N(x) - x}{\sqrt{D(x)}} = \frac{N_{\mathrm{fluc}}(x)}{\sqrt{D(x)}} \tag{17}$$

where

$$D(x) = \frac{\gamma(c)}{(c-1)x}\int_x^{cx}(N(y)-y)^2\,\mathrm{d}y = \langle N_{\mathrm{fluc}}^2(x)\rangle \tag{18}$$

where $\gamma(c)$ is a correction factor which goes to 1 when c goes to 1, to be explained below. By construction, $W(x)$ has a unit dispersion.

The Steiner conjecture (Steiner 1994, Aurich *et al* 1994) states that in ergodic (or more chaotic) systems the distribution of W is Gaussian, which means most random (in the sense of maximum entropy) under the prescribed value of unit dispersion, whilst in classically integrable systems it should be non-Gaussian. This is a non-trivial assertion, because absence of all correlations in the Poissonian spectrum of integrable systems might imply complete randomness at all scales, also such implicit in the distribution of W, where all scales are involved. Therefore at the largest scales, the behaviour of the chaotic spectra is more random than that of the integrable systems. This can be understood theoretically; see below. The experience so far supports the Steiner conjecture, including ours herein.

In this work we shall study the quantum mechanics of three billiard systems, rectangle, torus and circle billiard. In each case we solve the Helmholtz equation (Schrödinger equation), using the units $\hbar^2/2m = 1$,

$$\Delta\psi + E\psi = 0 \tag{19}$$

with the Dirichlet boundary conditions (vanishing ψ on the boundary) for rectangle and circle, and periodic boundary conditions on the torus. Then we can immediately write down the generalized Weyl formula (whose leading term is the Thomas–Fermi term obtained by equation (2)),

$$\overline{N}(E) = \frac{1}{4\pi}[\mathcal{A}E - \mathcal{L}\sqrt{E} + \mathcal{K}] \tag{20}$$

where $\mathcal{A}$ is the area of the billiard, $\mathcal{L}$ is its perimeter (circumference), which is, however, zero for the torus, and $\mathcal{K}$ contains curvature and corner corrections and is equal to $\pi/3$ for the rectangle, $\pi/2$ for the semicircle, and is zero for the torus. In reality, in the unfolding procedures (4) usually we shall work at such high energies, up to $x = \overline{N}(E) = 10^{11}$, that the leading Thomas–Fermi term of the Weyl formula (20) will be sufficient—but not for $W(x)$.

3. The rectangle billiards

3.1. The spectrum, unfolding, geometry and preliminaries

Using the units for our billiard systems of equation (19), $\hbar^2/2m = 1$, for the rectangle billiard with sides a and b we have the energy spectrum

$$E_{m,n} = \pi^2\left[\left(\frac{m}{a}\right)^2 + \left(\frac{n}{b}\right)^2\right] \tag{21}$$

where $m, n = 1, 2, \ldots$, and one parameter can be eliminated by unfolding and preserving the shape, for example by choosing $a = \pi$ and $b = \pi/\sqrt{\alpha}$, so that we obtain

$$E_{m,n} = m^2 + \alpha n^2 \tag{22}$$

and now α is the only shape parameter. The Weyl formula (20) then reads

$$\overline{N}(E) = \frac{\pi}{4\sqrt{\alpha}}E - \frac{1}{2}\left(\frac{1}{\sqrt{\alpha}} + 1\right)\sqrt{E} + \frac{1}{12}. \tag{23}$$

It is an interesting observation that at least two leading Weyl terms in (23) can be obtained purely geometrically by considering the plane (m, n), with $m, n = 1, 2, \ldots$. Inside the ellipse $E \leqslant E_{m,n}$ of equation (22) we have $\pi E/\sqrt{\alpha}$ grid points, and because of the positivity of m and n, only one quarter of them contribute to $\overline{N}(E)$. This gives the leading Weyl term. The next term stems from the fact that in calculating the above one quarter of the ellipse we have to subtract the two positive semiaxies, whose total length is exactly equal to the second Weyl term. Finally, we have to add something, because the contributions from $m, n = 0$ have been subtracted twice. However, this does not completely reproduce the third term in (23).

We shall examine the spectra up to as high energies as $\overline{N}(E) \approx 10^{11}$. We have always used at least the double precision on our computer, with about 15 valid digits, so that the resolution is only about 10^{-4} of the mean level spacing, which has been observed to affect the statistical results. In such cases we had to increase the precision to the quadruple precision (REAL*16). The calculations at such high energies are possible only because it is not necessary to memorize all the eigenvalues, but they can be easily and quickly calculated from the simple formula (22). For the delta statistics such high precision is not necessary, but the required CPU time is much larger than in calculations of the level spacings.

The preferred value of α will be $\alpha = \frac{\pi}{3}$, which is the same as in Casati *et al* (1985), and should be assumed if not stated otherwise. Hereafter we denote by E the unfolded energy, so its value is equal to $\overline{N}(E)$, i.e. the number of levels below E. We have chosen three energy intervals (windows) of size $E_{\text{start}}/1000$ and starting at E_{start}:

- 10^6 levels above $E_{\text{start}} = 10^9$, $\mathcal{O}_1$
- 10^7 levels above $E_{\text{start}} = 10^{10}$, $\mathcal{O}_2$
- 10^8 levels above $E_{\text{start}} = 10^{11}$, $\mathcal{O}_3$.

3.2. Level spacing distribution

In figures 1(a)–(c) we show $P(S)$ for the irrational rectangle with $\alpha = \pi/3$ for the windows $\mathcal{O}_1$, $\mathcal{O}_2$ and $\mathcal{O}_3$, respectively. It is seen that the agreement with the Poissonian statistics $P(S) = \exp(-S)$ is perfect. The bin size is $\Delta S = 0.001$.

At lower energies, say up to around $E = 100\,000$ we observe the statistically unexpectedly large fluctuations around the expected Poissonian value, as shown in figure 2, also in comparison with the results of Casati *et al* (1985). Unfortunately it is impossible to exactly reproduce their results because they neither give their numerical precision, nor describe the unfolding procedure (using the full Weyl formula as we do or only the leading Thomas–Fermi term). The qualitative behaviour can be confirmed, however, especially the size of fluctuations.

The impression in figures 1(a)–(c) is that the fluctuations around the theoretical Poissonian values decrease with energy, if the size of the bins $\Delta S = 0.001$ is fixed, and they certainly are within the statistically expected limits. In reality the picture is much more complicated. In figures 3(a)–(c) we show the results for $P(S)$ near $S = 0$ for the lowest 10^7, 10^8 and 10^9 levels, respectively, but such that the bin size ΔS shrinks with E so that in each bin we always have approximately $N_b \approx 10\,000$ level spacings, and therefore the expected statistical fluctuations should be roughly $\sqrt{1/N_b} \approx 0.01$. It can be seen that the observed fluctuations are clearly much bigger than their expected value and are approximately of the same size at all energies. We shall show below, that these fluctuations are due to the fact that the shape parameter α is always (at all energies) in the vicinity of sufficiently influencial rational values. This is thus definitely also the explanation of the fluctuations discovered and observed by Casati *et al* (1985). In order to ensure that our

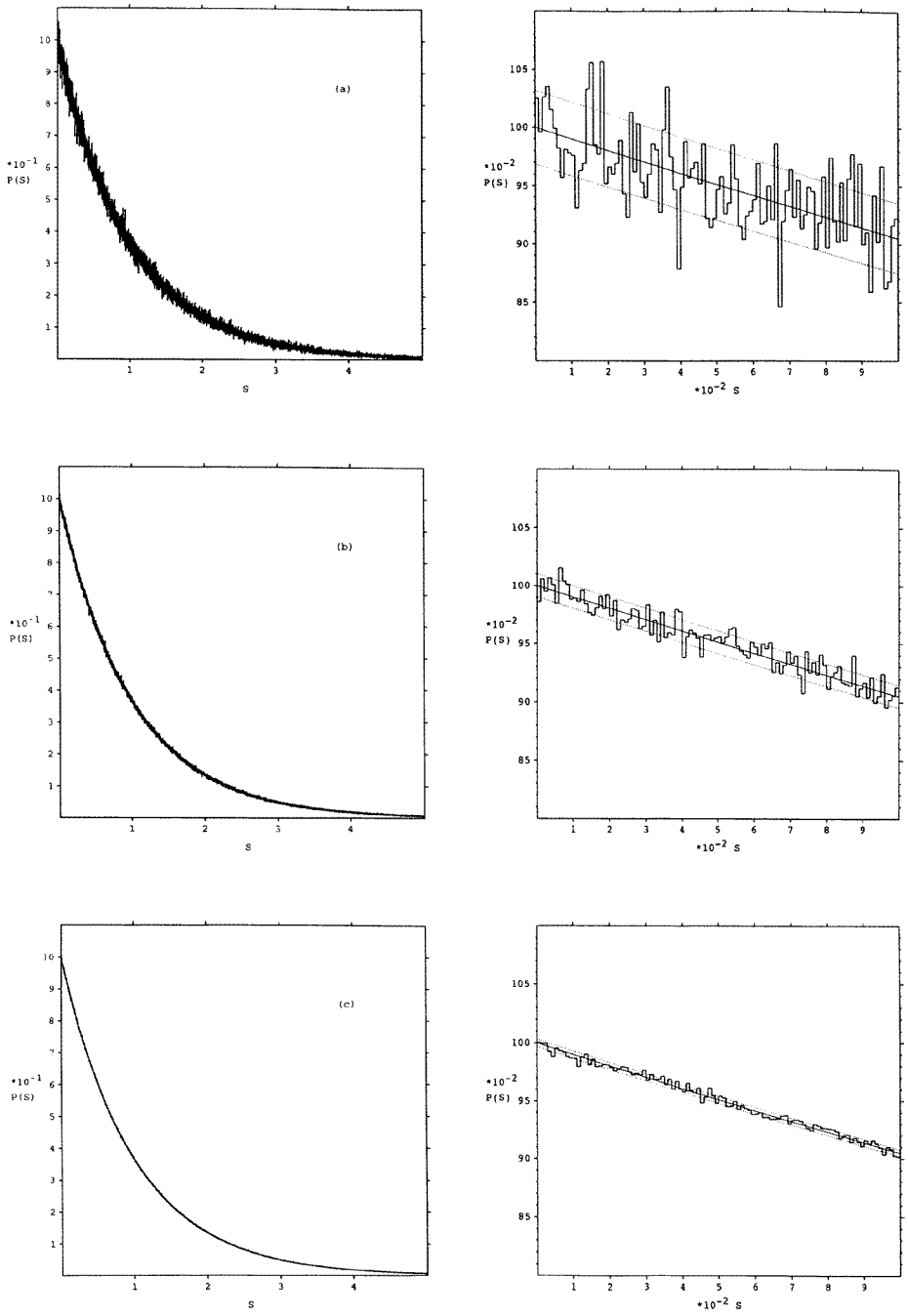

Figure 1. We show the level spacing distribution for the three windows $\mathcal{O}_1$–$\mathcal{O}_3$ in (a)–(c) respectively, in each case with the bin size $\Delta S = 0.001$. The shape parameter of the rectangle billiard is $\alpha = \pi/3$. The histograms clearly converge towards the theoretical value $P(S) = \exp(-S)$, and the size of the fluctuations also decreases. In the right hand picture in each case we show the enlarged part near $S = 0$, together with the statistically expected $\pm\sigma$ error (dotted) and theoretical Poissonian curve (full curve). The fluctuations here stay within the statistically expected range.

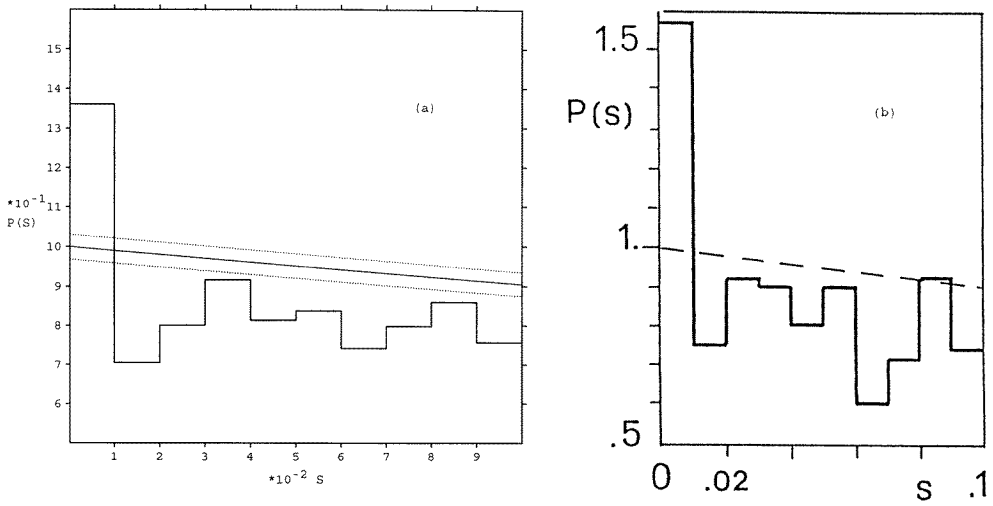

Figure 2. We show the results for the irrational rectangle $\alpha = \pi/3$ for (unfolded) energies up to 100 000, for $P(S)$ near $S = 0$. The fluctuations (a) are roughly as published by Casati *et al* (1985) in (b). We also plot the Poissonian curves (full in (a) and broken in (b)), and the expected $\pm\sigma$ standard deviation.

choice of α is not an unlucky choice we have checked the corresponding results for the most irrational value, namely the golden mean $\alpha = (\sqrt{5}-1)/2$. The results are practically unchanged and therefore we do not show them.

3.3. The rational rectangles

The rational rectangle billiards are defined by their shape parameter $\alpha = a^2/b^2$ being a rational number,

$$\alpha = \frac{q}{p} \tag{24}$$

where q and p are natural numbers without a common divisor. By unfolding the spectrum (22) with *only the leading term of the Weyl formula* (23) we then study the spectrum

$$E_{m,n} = \frac{\pi}{4\sqrt{pq}}[pm^2 + qn^2]. \tag{25}$$

At very high energies, say up to $\overline{N}(E) \approx 10^{11}$, and asymptotically when $E \to \infty$, such an unfolding procedure is certainly satisfactory. Then we immediately see that the energy levels appear only at the integer multiples of the quantity X,

$$X = \frac{\pi}{4\sqrt{pq}} \tag{26}$$

which has already been noticed by Berry and Tabor (1977). Therefore the level spacings S also take on only the integer multiple values of X. The distribution $P(S)$ is no longer smooth, but becomes a sum of the delta functions. Berry and Tabor (1977) introduced the discrete Poissonian model

$$P_X(n) = (1 - \exp(-X))\exp(-nX) \tag{27}$$

where $n = 0, 1, \ldots$, and tested it for $p = 5$ and $q = 7$ for the lowest 5000 levels and found a good agreement.

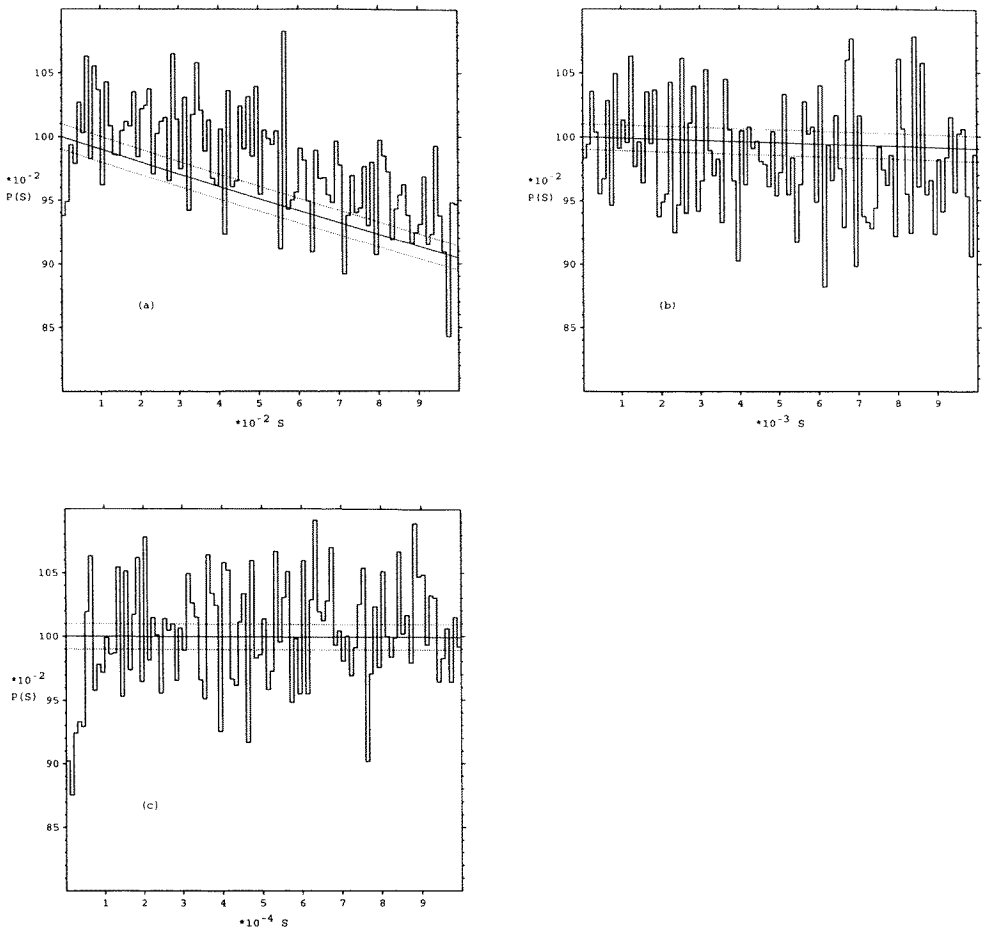

Figure 3. We show the histograms for the lowest 10^7, 10^8 and 10^9 levels, in (*a*), (*b*) and (*c*), respectively, near the origin $S = 0$. Here $\alpha = \pi/3$. The bin size shrinks with energy, such that in the bin there are always approximately $N_b \approx 10\,000$ spacings. The deviations are clearly much bigger than statistically expected $\pm\sigma$ error.

Our numerical calculations for $p = 21$ and $q = 22$ at high energies show that their model *does not* apply. In figure 4 we show the results for the three windows. The (discrete) distribution is certainly not Poissonian (27), but does not seem to change the shape with energy, which is, however, not true, as we shall see shortly. In fact, the probabilities (in delta spikes) decrease very slowly with energy, building up the main delta spike at $S = 0$ (which extends outside the plots), which is the only one that survives the limit $E \to \infty$.

Connors and Keating (1997) have recently studied the square billiard $p = q = 1$,

$$E_{m,n} = m^2 + n^2 \tag{28}$$

and demonstrated analytically the deviation from the Poissonian model. Let $r_2(n)$ denote the number of possibilities to write the natural number n as a sum of the squares of two natural numbers, which is nothing but the degeneracy of the (not unfolded, but actual) energy. With the definition

$$B_2(n) = 0 \text{ if } r_2(n) = 0 \text{ and } 1 \text{ otherwise} \tag{29}$$

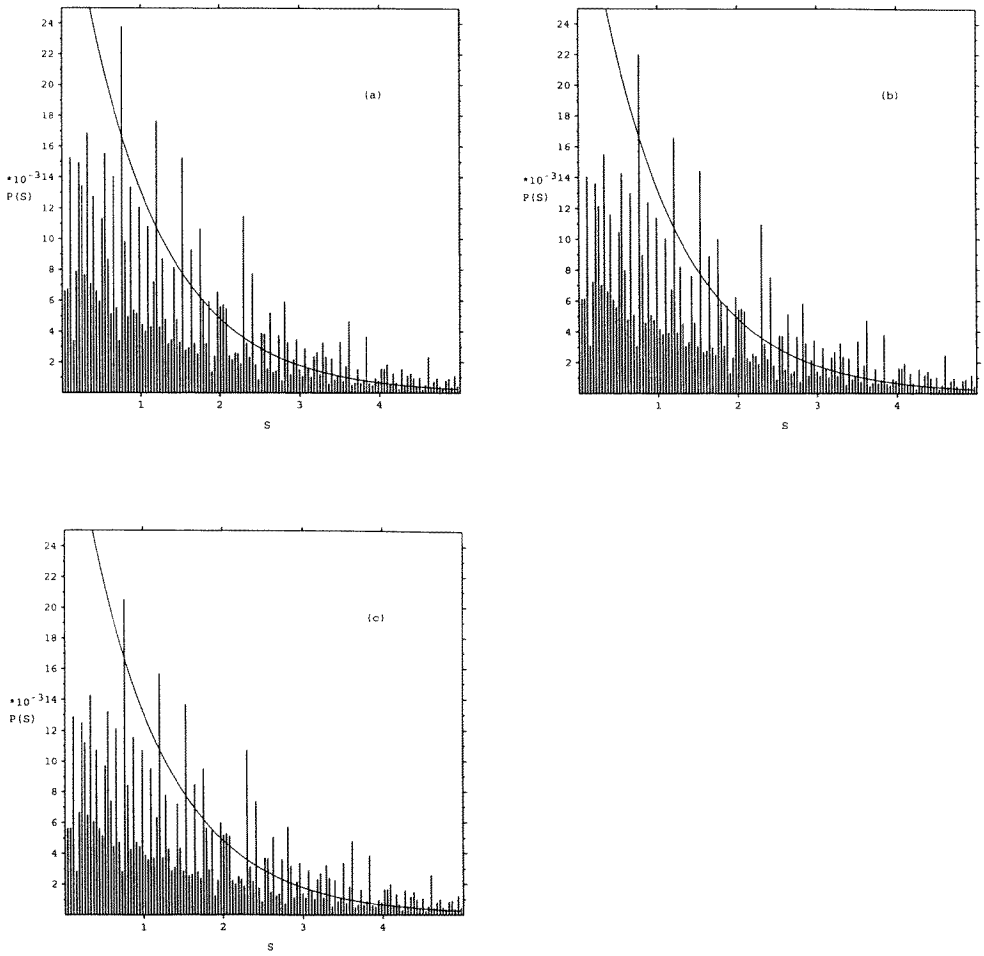

Figure 4. We show the discrete level spacing distributions for the rational rectangle billiard with $p = 21$ and $q = 22$ for the windows $\mathcal{O}_1$–$\mathcal{O}_3$ in (a)–(c), respectively. They obviously disagree with the Poissonian theoretical model (27). The delta spikes slowly decrease with energy, building up the asymptotically only one non-vanishing delta peak at $S = 0$. See text.

we can write $P(0) = P_X(0)$ as

$$P_X(0) = \frac{\Sigma_n(r_2(n) - B_2(n))}{\Sigma_n r_2(n)}. \tag{30}$$

The denominator is the number of all level spacings, which at large n is just equal to the number of all levels, in the numerator is the number of all terms contributing to $P_X(0)$; they are those whose energy can be expressed in at least two ways. It can be shown that the average value of $r_2(n)$ is equal to

$$\langle r_2(n)\rangle = \lim_{n\to\infty} \frac{r_2(n)}{n} = \frac{\pi}{4}. \tag{31}$$

Using the old result of Landau (1908)

$$\langle B_2(n)\rangle = \lim_{n\to\infty} \frac{B_2(n)}{n} = \frac{C}{\sqrt{\ln(n)}} \tag{32}$$

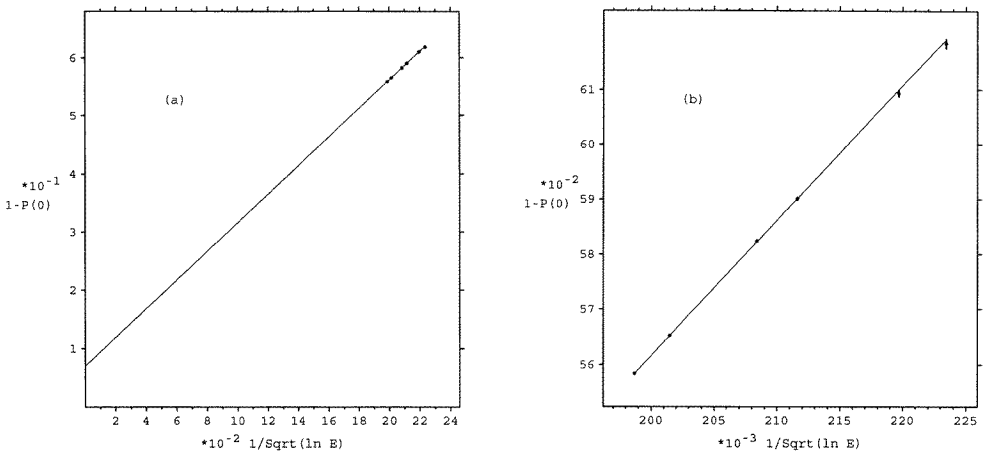

Figure 5. We test numerically the relationship (34) for $1 - P_X(0)$ for the rational rectangle with $p = 21$ and $q = 22$ for the energies 5×10^8–to 10^{11}. In (*b*) we show the enlarged region where the data lie. The agreement is seen to be very good. However, B_2 is not yet equal to zero as we expect to happen when we are sufficiently far in the asymptotic region of $\overline{N} \to \infty$. $B_2 \to 0$ implies $P_X(0) \to 1$.

yields

$$1 - P_X(0) = \frac{A}{\sqrt{\ln(\overline{N})}} \tag{33}$$

implying that $P(S)$ has asymptotically, when $E \to \infty$, $\overline{N} \to \infty$ only one delta peak, namely at $S = 0$, so that the limiting (discrete) level spacing distribution for the square billiard is just $P(S) = \delta(S)$, which is a little surprising.

Now we postulate that for a rational rectangle billiard with $p, q \neq 1$ the same functional dependence (33) applies as well. We assume the functional form

$$1 - P_X(0) = \frac{B_1}{\sqrt{\ln(\overline{N})}} + B_2 \tag{34}$$

and test it numerically, as shown in figure 5. The agreement is surprisingly good. However, the extrapolated constant B_2 is not yet seen to be zero, probably because we are not yet far enough in the asymptotic region (sufficiently large $\overline{N}$). Having observed the slow building up of the zero-spacing delta spike we also notice that the shape of the level spacing distribution as displayed in figure 4 seems to be roughly preserved with increasing energy. Therefore we have analysed the ratios $P_X(1)/P_X(2)$ and $P_X(28)/P_X(29)$, establishing their approximate constancy (independence of energy) as manifested in figure 6.

3.4. The neighbourhood of rational rectangles

It is interesting and important to see and understand what happens if we deform a rational rectangle billiard to an irrational one. The shape parameter α is an irrational number in a vicinity of the rational one q/p, written in the form

$$\alpha = \frac{q + \epsilon}{p}. \tag{35}$$

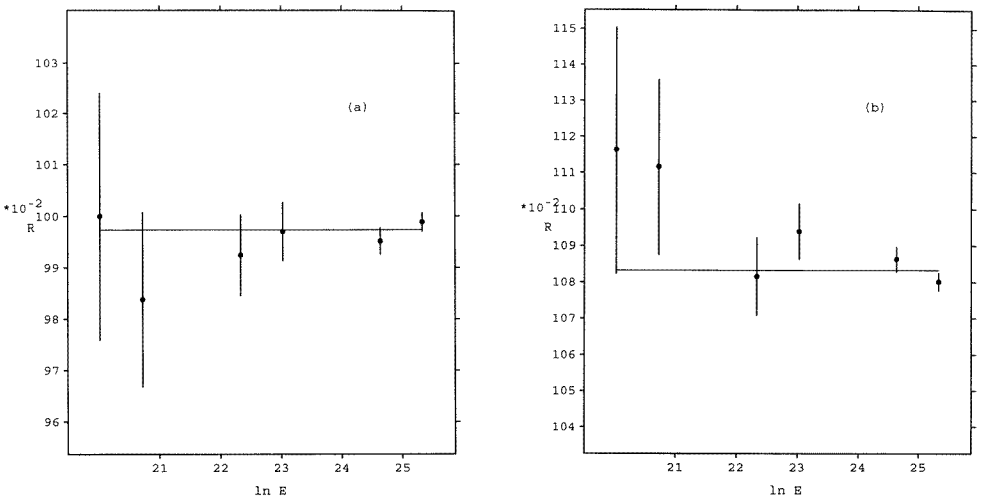

Figure 6. In (*a*) we show the ratio $P_X(1)/P_X(2)$ versus $\ln E$ and in (*b*) the ratio $P_X(28)/P_X(29)$ versus $\ln E$. Both seem to be approximately constant (independent of energy), implying the approximate preservation of the shape of $P_X(S)$ with the energy E.

The unfolded energy (using only the leading term of the Weyl formula (23), as before) reads

$$E = \frac{\pi}{4\sqrt{p(q+\epsilon)}}(pm^2 + (q+\epsilon)n^2). \tag{36}$$

To the first order in ϵ we write

$$E = E_{\text{rat}} + \delta E \tag{37}$$

where E_{rat} denotes the energy of the rational rectangle, equation (25), and

$$\delta E = \epsilon\left(\beta n^2 - \frac{E}{2q}\right) \qquad \beta = X = \frac{\pi}{4\sqrt{pq}}. \tag{38}$$

We calculate the distribution of the energy shift $\mathrm{d}w/\mathrm{d}\delta E$ near the energy $E \approx E_{\text{rat}}$ when the rectangle is slightly distorted away from its rational shape. One can write

$$\frac{\mathrm{d}w}{\mathrm{d}\delta E} = \frac{\mathrm{d}w}{\mathrm{d}n}\frac{\mathrm{d}n}{\mathrm{d}\delta E} \qquad \frac{\mathrm{d}n}{\mathrm{d}\delta E} = \frac{C}{\sqrt{\delta E + \frac{\epsilon E}{2q}}}. \tag{39}$$

The right-hand expression is obtained from (38), and $\mathrm{d}w/\mathrm{d}n$ is the distribution of the quantum number n near the given energy E. By geometrical considerations one finds the distribution of the levels along an arc of the contour $E = \beta(pm^2 + qn^2) = \text{constant}$, namely

$$\frac{\mathrm{d}w}{\mathrm{d}l} = \frac{D}{|\nabla E|} \qquad |\nabla E| = 2\beta\sqrt{p^2m^2 + q^2n^2} \tag{40}$$

where the latter result follows by considering the area of the space (m, n) in which the levels are uniformly distributed which is spanned by the given arc of length $\mathrm{d}l$ when the energy E is slightly increased. Using the relationships $\mathrm{d}l^2 = \mathrm{d}m^2 + \mathrm{d}n^2$ and $\mathrm{d}E = \frac{\partial E}{\partial m}\mathrm{d}m + \frac{\partial E}{\partial n}\mathrm{d}n = 0$, we find

$$\frac{\mathrm{d}l}{\mathrm{d}n} = \frac{1}{pm}\sqrt{p^2m^2 + q^2n^2}. \tag{41}$$

From the last two equations one concludes

$$\frac{\mathrm{d}w}{\mathrm{d}n} = \frac{\mathrm{d}w}{\mathrm{d}l}\frac{\mathrm{d}l}{\mathrm{d}n} = \frac{D}{2\beta pm} \qquad m = \sqrt{\frac{E}{\beta p} - \frac{q}{p}n^2} \tag{42}$$

and upon inserting this into equation (39) and expressing n in terms of δE, we finally obtain the probability distribution of the energy shifts δE,

$$\frac{\mathrm{d}w}{\mathrm{d}\delta E} = \frac{1}{\pi}\frac{1}{\sqrt{\Gamma^2 - (\delta E)^2}} \qquad \Gamma = \frac{\epsilon E}{2q} \tag{43}$$

where the final value of the proportionality constant $\propto C$, D has been set by normalizing the final probability distribution. Note that the only parameter in this distribution is $\Gamma = \epsilon E/2q$, which is practically constant for the energy E inside a spectral stretch, such as in our three windows $\mathcal{O}_1, \mathcal{O}_2, \mathcal{O}_3$ which have the length $E_{\mathrm{start}}/1000$.

From the calculation of the (distribution of the) energy shifts we now calculate the distribution of the level spacing shifts δS, defined by

$$S = S_{\mathrm{rat}} + \delta S \tag{44}$$

where S_{rat} is the level spacing of the rational billiard. We are going to study its broadening when the rectangle is distorted away from the rational shape according to (35). Of course, the δS is the difference of the two energy shifts,

$$\delta S = \delta E_2 - \delta E_1. \tag{45}$$

Clearly, we have to find the distribution of the difference of two variables δE_1 and δE_2, for which we assume that they are statistically independent and have the same distribution (43). Then we have

$$\frac{\mathrm{d}w}{\mathrm{d}\delta S} = \int \frac{\mathrm{d}w}{\mathrm{d}\delta E}(x)\frac{\mathrm{d}w}{\mathrm{d}\delta E}(x + \delta S)\,\mathrm{d}x \tag{46}$$

the result being even function of δS. For the positive values of δS it reads

$$\frac{\mathrm{d}w}{\mathrm{d}\delta S} = \frac{1}{\pi^2}\int_{-\Gamma}^{\Gamma-\delta S} \frac{\mathrm{d}x}{\sqrt{(\Gamma^2 - x^2)(\Gamma^2 - (x+\delta S)^2)}} \tag{47}$$

which can be expressed in terms of the elliptic functions (Gradshteyn and Ryzhik 1994, p 290),

$$\frac{\mathrm{d}w}{\mathrm{d}\delta S} = \frac{1}{\pi^2\Gamma}F\left(\frac{\pi}{2}, \sqrt{1 - \left(\frac{\delta S}{2\Gamma}\right)^2}\right) = \frac{1}{\pi^2\Gamma}K\left(\sqrt{1 - \left(\frac{\delta S}{2\Gamma}\right)^2}\right). \tag{48}$$

An inspection of numerical profiles of the $\mathrm{d}w/\mathrm{d}\delta S$ distribution near a rational S_{rat} shows that indeed the distribution is symmetric (even in δS), at sufficiently large p, q. At lower values of p, q we observe strong asymmetry, which is caused by the fact that we have neglected the degeneracies, as will soon become clear. Indeed, Poissonian spectra have many degeneracies, and non-generic rational billiards even more so. It is therefore quite essential—at least in our rectangle billiards—to take into account all multiplets (=degeneracies of higher order), to achieve agreement with the numerical values of $\mathrm{d}w/\mathrm{d}\delta S$ around $S = S_{\mathrm{rat}}$.

In figure 7 we show a sketch of the situation in which there are two consecutive energy contours at $\epsilon = 0$ (full curve, with a pair of degenerate levels, followed by a triplet at slightly higher energy, namely by S_{rat} higher) and the shifted energy contours (broken curve, $\epsilon \neq 0$). By l we shall denote the multiplet ($l = 1$ for singlet, $l = 2$ for doublet, $l = 3$ for triplet, and

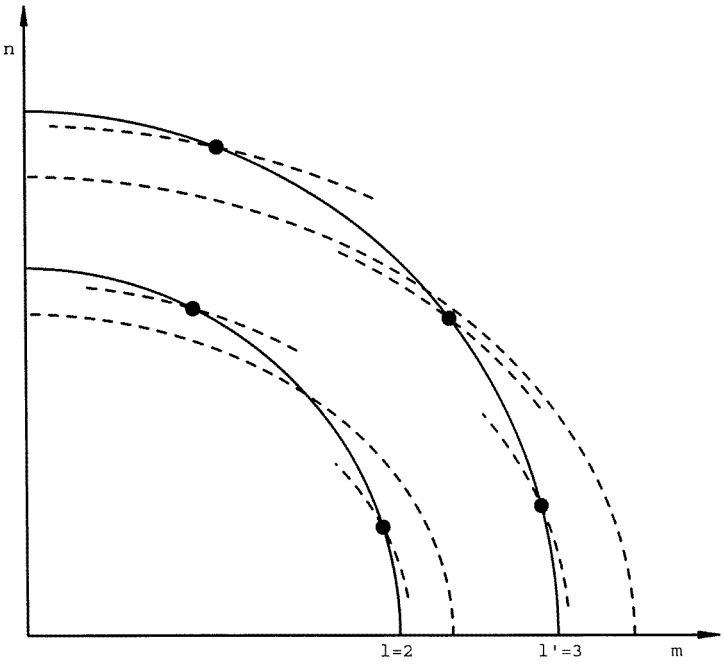

Figure 7. We show the sketch of the situation in the plane (m, n) of having two consecutive energy curves at $\epsilon = 0$ (full curve, with a pair of degenerate levels, followed by a triplet at slightly higher energy, namely by $S_{\rm rat}$ higher) and the distorted energy contours (broken lines, $\epsilon \neq 0$). By l we shall denote the multiplet ($l = 1$ for singlet, $l = 2$ for doublet, $l = 3$ for triplet, and so on). In general members of a multiplet are shifted to slightly different distorted energy contours (broken) when $\epsilon \neq 0$.

so on), and by $u(l)$ we shall denote the relative fraction of all the l multiplets within the number of all multiplets. Thus $u(l) =$ (number of l multiplets)/(number of all multiplets). Then by δE_i^l we shall denote the shifts of the levels in the lower energy shell (with l levels, see figure 7), and by δE_i^u those of the higher one (l' multiplet). Clearly, with the known energy shifts we calculate the shift of the level spacing $S_{\rm rat}$ as

$$\delta S = \min_{i=1,\ldots,l'}(\delta E_i^u) - \max_{i=1,\ldots,l}(\delta E_i^l) \tag{49}$$

or in another notation

$$\delta S = \delta E_r^u - \delta E_t^l \qquad (\delta E_r^u \leqslant \delta E_i^u, \forall i \neq r) \wedge (\delta E_t^l \geqslant \delta E_i^l, \forall i \neq t). \tag{50}$$

The distribution of the level spacing shifts between two multiplets l and l' can then be written down symbolically

$$W_{l,l'} = \sum_r \sum_t \int \boldsymbol{D}(\delta E_r^u - \delta E_t^l - \delta S)\mathrm{Prob}(\delta E_r^u \leqslant \delta E_i^u)\mathrm{Prob}(\delta E_t^l \geqslant \delta E_i^l) \times w(\delta E_r^u) w(\delta E_t^l) \mathrm{d}\delta E_r^u \mathrm{d}\delta E_t^l \tag{51}$$

where $\boldsymbol{D}(x)$ is the Dirac delta function here, to be distinguished from the notation δ reserved for the shifts. We now measure the energy shifts in units of Γ from equation (43), so that in these units

$$\mu(\delta E) = \frac{\mathrm{d}w}{\mathrm{d}\delta E} = \frac{1}{\pi}\frac{1}{\sqrt{1-(\delta E)^2}}. \tag{52}$$

It is easy then to calculate

$$\mathrm{Prob}(\delta E_r^u \leqslant \delta E_i^u) = \prod_{i\neq r} \int_{\delta E_r^u}^{1} \mu(\delta E_i^u)\mathrm{d}\delta E_i = \left(\frac{1}{2} - \frac{1}{\pi}\arcsin \delta E_r^u\right)^{l'-1} \tag{53}$$

and

$$\mathrm{Prob}(\delta E_t^l \geqslant \delta E_i^l) = \prod_{i\neq t} \int_{-1}^{\delta E_t^l} \mu(\delta E_i^l)\mathrm{d}\delta E_i = \left(\frac{1}{2} + \frac{1}{\pi}\arcsin \delta E_t^l\right)^{l-1}. \tag{54}$$

The quantities (51) become

$$W_{l,l'} = ll' \int_a^b \mu(\delta E)\mu(\delta S + \delta E)\left(\frac{1}{2} + \frac{1}{\pi}\arcsin \delta E\right)^{l-1} \times \left(\frac{1}{2} - \frac{1}{\pi}\arcsin(\delta S + \delta E)\right)^{l'-1} \mathrm{d}\delta E \tag{55}$$

where the integration limits are

$$\begin{aligned} (a, b) &= (-1 - \delta S, 1) \qquad \text{if } \delta S < 0 \\ (a, b) &= (-1, 1 - \delta S) \qquad \text{if } \delta S > 0. \end{aligned} \tag{56}$$

Now by substitution $\delta E' = \delta E + \delta S/2$, and by rearranging one finds

$$W_{l,l'} = ll' \int_{-1+|\delta S|/2}^{1-|\delta S|/2} \mathrm{d}\delta\, E' \mu\left(\frac{\delta S}{2} + \delta E'\right)\mu\left(\frac{\delta S}{2} - \delta E'\right) \times \left(\frac{1}{2} - \frac{1}{\pi}\arcsin\left(\frac{\delta S}{2} - \delta E'\right)\right)^{l-1}\left(\frac{1}{2} - \frac{1}{\pi}\arcsin\left(\frac{\delta S}{2} + \delta E'\right)\right)^{l'-1} \tag{57}$$

and we obtain the final general formula for the level spacing shift distribution, denoted by $\mathrm{d}w/\mathrm{d}\delta\, S$,

$$\frac{\mathrm{d}w}{\mathrm{d}\delta S} = \sum_l \sum_{l'} u(l)u(l')W_{l,l'}(\delta S) \tag{58}$$

where $W_{l,l'}$ is given in equation (57). This final result can now be tested against the numerical (empirical) distribution. Whilst $W_{l,l'}$ are calculated in a straightforward manner, the quantities $u(l)$ must be known either theoretically or at least empirically. In the former case one has to solve difficult problems in the number theory, whilst in the latter case one can easily obtain them by inspecting the spectrum and counting the multiplets. This is what we have done.

In figure 8 we show the case of the irrational triangle close to the rational one, namely $p = 21$, $q = 22$, and $\epsilon = 10^{-12}$. The data are taken from the window $\mathcal{O}_3$, i.e. $E_{\mathrm{start}} = 10^{11}$, and we have 10^8 levels. The level spacing shift δS is measured in units of 2Γ, where $\Gamma = \epsilon E/(2q)$. As we clearly see we have a logarithmic singularity at $\delta S = 0$ (typical of the elliptic functions) and discontinuities at the limits of definition $\delta = \pm 2\Gamma$. The agreement of data with the theoretical prediction of equation (58) is very good. The distribution is strongly asymmetrical, which is a consequence of the existence of the multiplets with $l = 2$ and higher. Indeed, if we go to the rational rectangles of higher degree, for example $p = 339$, $q = 355$, we find the trend to symmetrical distribution predicted by (47) or (48), as shown in figure 9. This trend towards symmetry is precisely due to the smaller influence of multiplets $l \geqslant 2$, which are not accounted for in deriving the equations (47) and (48) as a special case $l = 1$ and $l' = 1$ of equation (58).

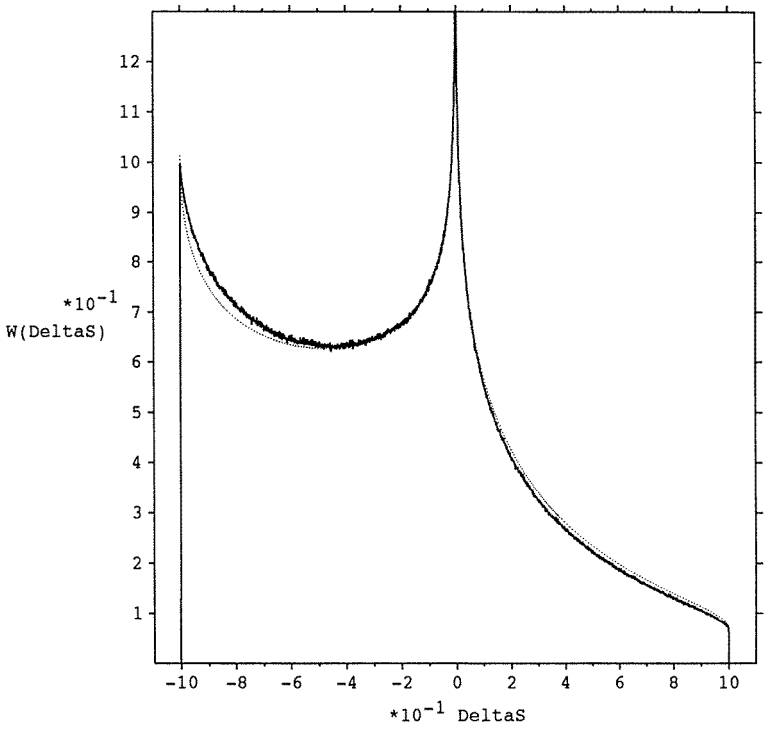

Figure 8. The spacing shift $\delta S = S - S_{\rm rat}$ distribution for the irrational triangle $p = 21$, $q = 22$ and $\epsilon = 10^{-12}$ (see equation (35)). The data are taken from the window $\mathcal{O}_3$, i.e. $E_{\rm start} = 10^{11}$, and we have approximately 10^8 levels in the statistics. δS is measured in units of 2Γ, where $\Gamma = \epsilon E/(2q)$ and is constant for all objects in the histogram. The agreement of data with the theoretical prediction (58) (dotted) is very good. The distribution is strongly asymmetrical which is due to the existence of the multiplets $l \geqslant 2$. The observed deviations are probably due to the correlations between the multiplets and among the members of a multiplet, which are not accounted for in (58). Also, the corrections in ϵ higher than linear (see equation (38)) are not accounted for, but are probably of lesser importance than the correlations in this context.

We should comment that the small deviations seen in figure 8 are definitely due to the not-accounted-for correlations within the l-multiplets. Probably the effect of neglecting terms higher than linear in ϵ (see equation (38)) is smaller and less important in this context. This has been confirmed by random generation of the multiplets where a perfect agreement with (58) has been found. We have not pursued these theoretical refinements any further.

3.5. The fluctuations in $P(S)$ in the vicinity of the rational rectangles

Now we are in the position to explain the large fluctuations observed in $P(S)$ for *the irrational rectangles*, with $\alpha = (q + \epsilon)/p$ of equation (35), as uncovered in figures 2 and 3. From the analysis of section 3.4 it is clear that the criterion for the closeness to a rational rectangle billiard must be qualified in terms of the two quantities Γ and $\beta = X$, equations (38), (39), (47), (48) and (58). The spectrum will obviously exhibit the properties of the rational billiards whenever the rational spacing of level spacings $\beta = X$ will be larger than the half-width 2Γ of the spacings shift distribution:

$$2\Gamma \leqslant \beta = X \tag{59}$$

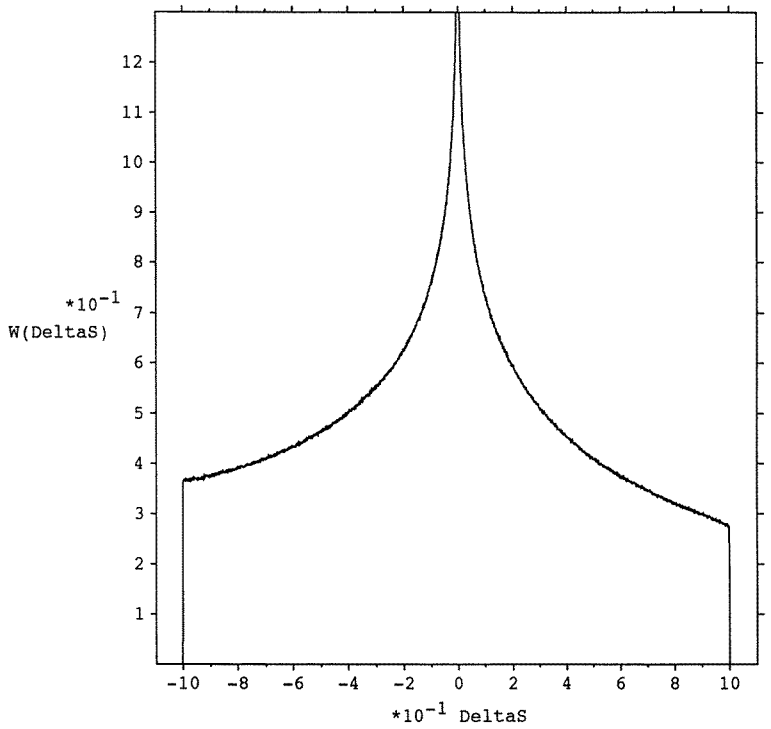

Figure 9. As in figure 8 but with $p = 339$ and $q = 355$. The distribution now is almost symmetrical, which is a consequence of the smaller influence of the multiplets $l \geqslant 2$. Therefore the general formula (58) is well approximated by the symmetrical one (even in δS) in equation (48), because $l = l' = 1$ is a good approximation. The agreement with equation (58) is now perfect.

or

$$\frac{\epsilon E}{q} \leqslant \frac{\pi}{4\sqrt{pq}}. \tag{60}$$

On the other hand, the scale on which we observe $P(S)$ must also be sufficiently small in order to enable the observability of the almost-rationality of α: the width of the ΔS-intervals (bins) must be smaller than β,

$$\Delta S < \beta. \tag{61}$$

However, the size of the bins may not be too small, since otherwise we lose the statistical significance. We want N_b level spacings per one bin of size ΔS. Since the unfolded energy E is (on the average) equal to the number of all levels, and this is also the number of all level spacings, and since all the spacings are effectively distributed within the interval of S of order unity (exponential Poissonian decay at large S), we have the condition

$$\Delta S \approx \frac{N_b}{E}. \tag{62}$$

Therefore our equation (61) can be rewritten as

$$\frac{N_b}{E} < \frac{\pi}{4\sqrt{pq}} \tag{63}$$

where E is the unfolded energy (roughly equal to the number of levels, starting from the ground state).

In equation (63) one can recognize the criterion for the largest pair (p, q) that can be observed at the given energy E, whilst in equation (60) we identify the condition for the largest ϵ to be observed as a rational-like $P(S)$. So we ask the question: What is the probability that we can find—up to the largest p—a suitably small ϵ? From the definition of α and ϵ in (35) one has

$$\epsilon = \alpha p - [\alpha p] \tag{64}$$

where $[x]$ denotes the integer part of the real number x. It is known from the number theory (Hardy and Wright 1983) that ϵ is uniformly distributed on the interval $[0, 1)$ when all possible p are considered provided α is an irrational number. We shall assume that ϵ' are indeed uniformly distributed on the stated interval (which is certainly acceptable, since the algorithm (64) is the basis of the congruent generators of random numbers).

The probability of finding ϵ', at fixed value of p, smaller than the maximal allowed ϵ of equation (60) is just equal to ϵ. The probability of finding at least one such ϵ' with all possible p' smaller than the maximal allowed one p, can be estimated in the following way. $(1 - \epsilon)$ is the probability that we cannot find a suitable ϵ' for a chosen p', and therefore the probability of not finding a suitable ϵ' *for all possible* $p' \leqslant p$ is just equal to $(1 - \epsilon)^p$. The probability of finding at least one suitable ϵ' is complementary to it, so equal to

$$W_\epsilon^p = 1 - (1 - \epsilon)^p. \tag{65}$$

Now using the estimates for the largest possible ϵ and largest possible p, from equations (60) and (63), considering $q \approx p$ and neglecting all the constants (of order 1), we obtain (assuming small product ϵp),

$$W_\epsilon^p \approx \epsilon p \approx \frac{1}{N_b}. \tag{66}$$

The estimate of this probability is not a sharp number but rather an assessment of the order of magnitude and it certainly is not a probability for fluctuations. The influence of the rational numbers does not disappear abruptly but continuously, and also we do not detect only the presence of one nearby rational number but of many of them. Therefore equation (66) is a criterion rather than a probability for the fluctuations in $P(S)$ to occur. As such it is obviously independent of the energy E. It does not directly predict the existence of fluctuations, but tells us, that the fluctuations must exist at any energy E if they are observed at certain energy, provided we keep the number of spacings in a bin constant and equal to N_b. This phenomenon is clearly manifested in figures 2 and 3. In the latter we have $N_b = 10\,000$ data per bin and we see that the fluctuations are much larger than the statistically expected relative error of $1/\sqrt{N_b} = 0.01$. In the analysis of Casati *et al* (1985) there were only $N_b = 1000$ objects per bin, so according to equation (66) the estimated fluctuations should be bigger by a factor of 10 rather than $\sqrt{10}$, which is confirmed in figure 2.

On the other hand, if the bin size ΔS is kept fixed, the estimate (66) becomes

$$W_\epsilon \approx \frac{1}{E \Delta S} \tag{67}$$

and it is now obvious that the fluctuations decrease with increasing energy (which also is the semiclassical limit).

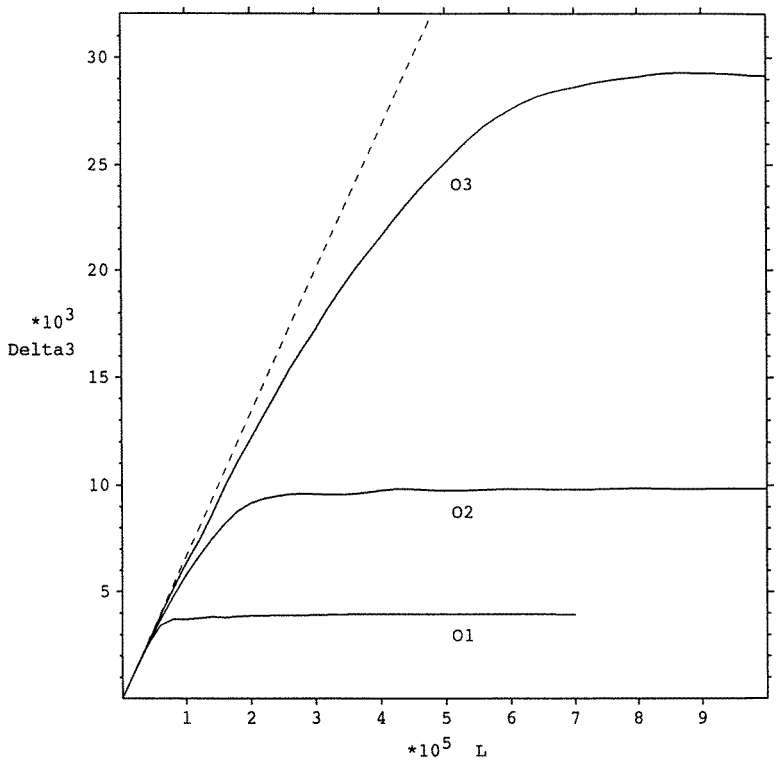

Figure 10. We show the delta statistics $\Delta(L)$ for the three energy windows $\mathcal{O}_1, \mathcal{O}_2$ and $\mathcal{O}_3$, defined in section 3.1, for the irrational rectangle with $\alpha = \pi/3$.

3.6. Long-range correlations

The level spacing distribution $P(S)$ contains information on short-range correlations, whilst the long-range correlations can be most conveniently analysed by the delta statistics $\Delta(L)$, or more generally, by the $E(k, L)$ statistics. For definitions and mutual relations see section 2.

In figure 10 we show $\Delta(L)$ for the three energy windows $\mathcal{O}_1 - \mathcal{O}_3$ defined in section 3.1. Up to $L \leqslant L_{\max}$ we see good agreement with the Poissonian value $L/15$. The saturation appears at $L \geqslant L_{\max}$, where $L_{\max} = \overline{h}/(T_0\langle\delta E\rangle)$ is dynamically determined according to Berry's (1985) theory of spectral rigidity (based on the Gutzwiller periodic orbit theory). Here T_0 is the period of the shortest classical periodic orbit, and scales $T_0 \propto 1/\sqrt{E}$, whilst $\langle\Delta E\rangle$ is the mean energy level spacing, which according to the Weyl formula (20) is independent of the energy in the limit of sufficiently large E. Consequently,

$$L_{\max} \propto \sqrt{E}. \tag{68}$$

The estimate agrees well with our data in figure 10, and also the estimated saturation value Δ_∞,

$$\Delta_\infty = 0.0947\sqrt{E}. \tag{69}$$

In the window $\mathcal{O}_3$ the agreement of $\Delta(L)$ with the data is at least up to $L \approx 10^3$ and increases with energy. Thus in the strict semiclassical limit of $E \to \infty$ we indeed have the Poissonian behaviour at an arbitrarily large scale L.

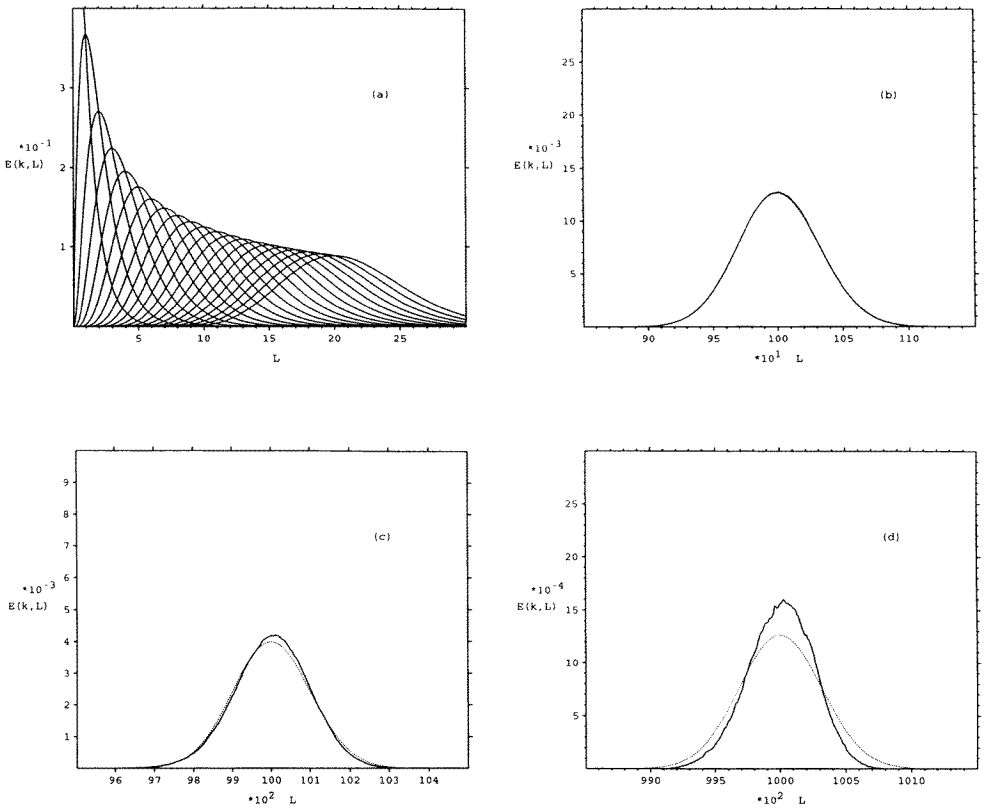

Figure 11. The functions $E(k, L)$ for the irrational rectangle billiard $\alpha = \pi/3$, for the highest energy window $\mathcal{O}_3$ defined in section 3.1. In (*a*) we have $0 \leqslant k \leqslant 20$, (*b*) $k = 10^3$, (*c*) $k = 10^4$, and (*d*) $k = 10^5$. The agreement for k and L up to approximately 10^3 is excellent.

In figure 11 we show the $E(k, L)$ statistics in the highest energy window $\mathcal{O}_3$, and the agreement with Poissonian theory is excellent up to the values of k of order $k_{\max} \approx L_{\max} \approx 10^3$. At higher k, $k > k_{\max}$, the accuracy breaks down for the same reasons as in $\Delta(L)$ for $L > L_{\max}$. Of course, there is a connection between the two quantities as explained in section 2.

When we return to the rational rectangles, we expect again some deviations from the Poissonian values, just in analogy with $P(S)$ described earlier. We consider again the rational case $\alpha = \frac{22}{21}$, so $p = 21$, $q = 22$. In figure 12 one can see that $\Delta(L)$ rises more steeply than Poissonian at small L, just due to the abundant degeneracies, then it becomes quite Poissonian, and saturates at a certain value Δ_∞ at large $L > L_{\max}$. In figure 13 we also show the $E(k, L)$ statistics. Similarly, for small k and L we expect deviations from the Poissonian values (12). Indeed, Connors and Keating (1997) have shown that the average square of degeneracy for the square $p = q = 1$ is equal to

$$\langle r_2^2(n)\rangle = A \ln(n) \tag{70}$$

and from our experience with $P(S)$ we can expect something similar for $p, q \neq 1$. Therefore at

$$k, L \leqslant \sqrt{\ln(n)} \tag{71}$$

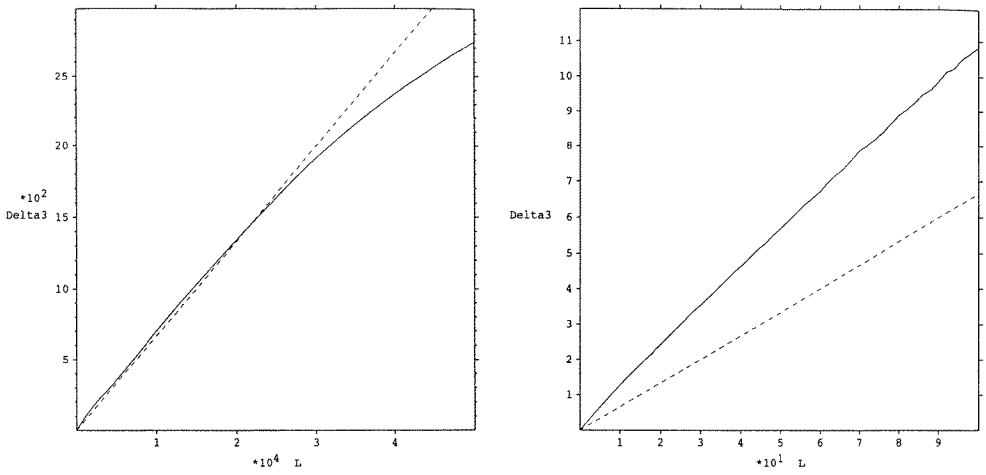

Figure 12. $\Delta(L)$ statistics for the rational rectangle billiard $\alpha = \frac{22}{21}$ in the energy window $\mathcal{O}_1$ defined in section 3.1. On the right we show a magnified part at small L.

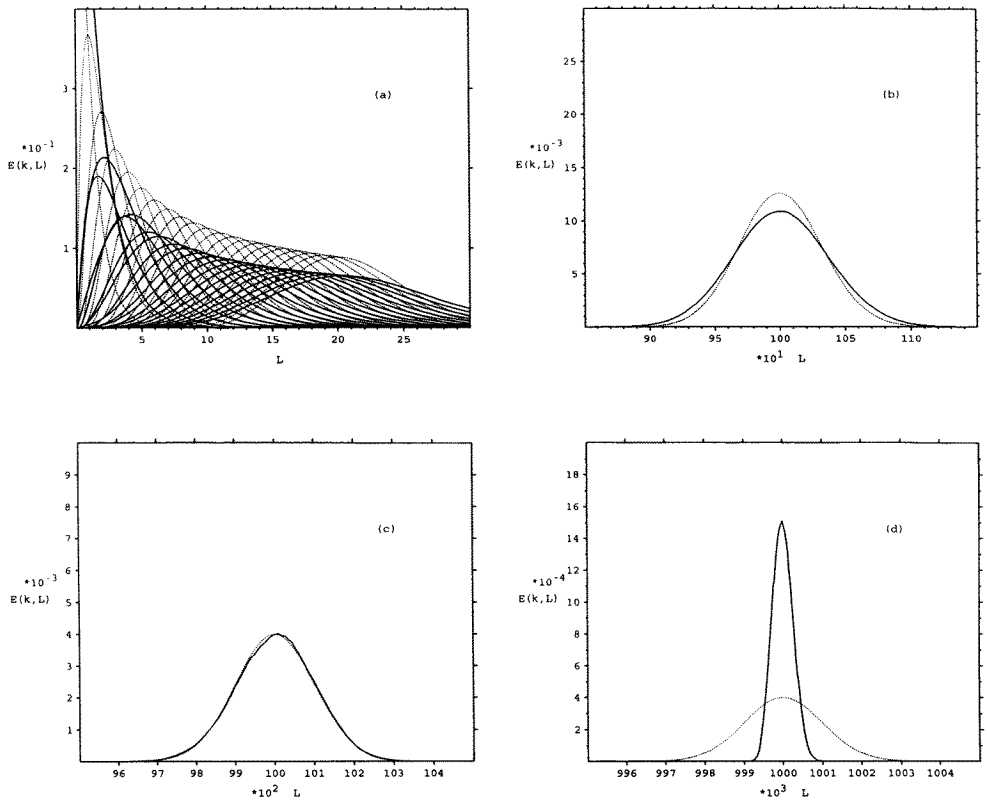

Figure 13. $E(k, L)$ statistics for the rational rectangle $\alpha = \frac{22}{21}$: $0 \leqslant k \leqslant 20$ in (a), $k = 10^3$ in (b), $k = 10^4$ in (c) and $k = 10^6$ in (d), all for the energy window $\mathcal{O}_3$ defined in section 3.1. The agreement is good only near $L \approx k \approx 10^4$.

we predict deviations of data from the Poissonian values, which is confirmed in figure 13. For larger k there is some good agreement, and $E(k, L)$ curves are more similar to the Poissonian curves, but nevertheless a little wider, which again is precisely due to the degeneracies and clustering of the levels. Since after unfolding the average spacing is 1, the clustering implies that the average distance between the clusters must increase, which means that $E(k, L)$ with maximum at $L \approx k$ must widen. For the intermediate k, but still smaller than $k_{\max}$ we find considerable agreement with the Poissonian values, whilst for $k \approx k_{\max} \approx L_{\max}$ the functions $E(k, L)$ become narrower than the Poissonian, quite similar to in the irrational billiards, which has the explained dynamical origin (Berry 1985). It should be emphasized again, however, that for sufficiently large L, in the limit $E \to \infty$, implying $L_{\max} \propto \sqrt{E} \to \infty$, the $E(k, L)$ statistics behave in the Poissonian way (12), and so do all other statistical measures, since they are all connected to (expressible by) them.

3.7. Reduced mode number fluctuations

In section 2 we introduced and defined the reduced mode number $W(x)$, equation (17), which is regarded as a stochastic variable having a certain limiting probability distribution $P(W)$ when the number of objects contained in the statistics goes to infinity. This quantity is interesting because in a sense it contains information for the spectral statistical measures at all scales. What laws can we expect for $P(W)$ for classically integrable system with Poissonian statistics (up to the range $L \leqslant L_{\max}$), and what statistics in other systems, generic, and fully chaotic?

We have seen that classically integrable systems like our irrational rectangles exhibit Poissonian statistics up to the energy ranges $L \leqslant L_{\max}$, where the dynamical saturation effect (Berry 1985) sets in. It is also important to recall that in the semiclassical limit $E \to \infty$ (or in the original physical units $\overline{h} \to 0$), $L_{\max}$ also goes to infinity, so that Poissonian behaviour can be found everywhere and on arbitrarily large scales. Also, it is intuitively quite obvious that the complete randomness of the Poissonian spectra, absence of all correlations, should imply a Gaussian $P(W)$ (cf Steiner 1994, Aurich *et al* 1994), with prescribed dispersion, in our units unit dispersion. Given the prescribed dispersion (variance) the Gaussian distribution $P(W)$ is the one having the largest entropy, so corresponds to the most random process $W(x)$. In the literature (Bleher *et al* 1993) we have definite examples of non-Gaussian $P(W)$ for classically integrable systems, which means also non-Poissonian $P(W)$. According to the Steiner conjecture the distribution should be non-Gaussian except if and only if the underlying classical system is fully chaotic (ergodic, mixing and K). So why is non-Gaussian (and thus non-Poissonian) behaviour of $P(W)$ now compatible with the Poissonian statistics up to $L \leqslant L_{\max}$?

The puzzling paradox we are facing here can be easily resolved. A short calculation shows that for the largest (unfolded) energy $L_{\max} = \sqrt{E} \ll E = \overline{N}(E)$. This means that when studying the correlations at scales L equal up to the maximum energy of the spectral stretch, *we are always in the saturation regime* of $L \geqslant L_{\max}$, and therefore we cannot observe anything universal, *except for the extreme case of having the maximum entropy distribution, described by the Gaussian $P(W)$, corresponding to the classically ergodic systems*. This is precisely the Steiner Conjecture (1994). (See also the recent review by Steiner and co-workers (Aurich *et al* 1997).)

Since this criterion is so important we want to express it in terms of the original physical units for two-dimensional billiard systems:

$$L_{\max} = \frac{\overline{h}}{T_0 \langle \Delta E \rangle} \leqslant \overline{N}(E) \tag{72}$$

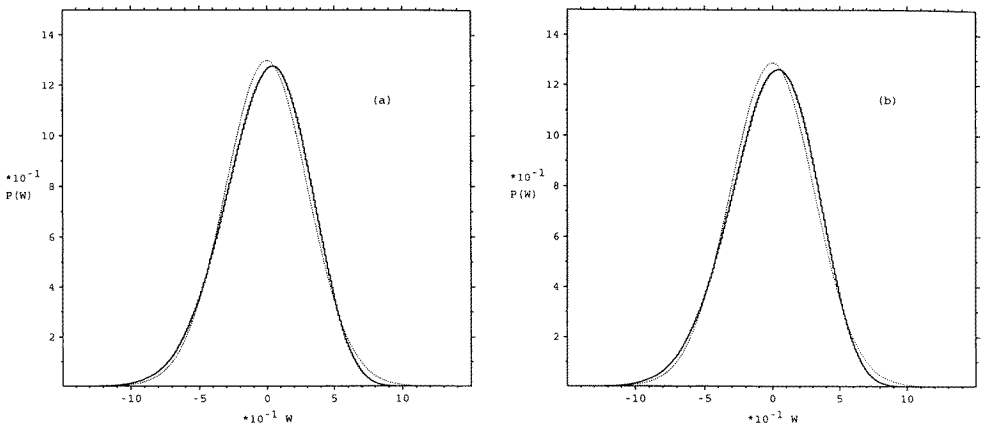

Figure 14. We show the reduced mode number probability distribution $P(W)$, defined in equation (17), for two irrational rectangle billiards, $\alpha = \pi/3$ in (a) and $\alpha = (\sqrt{5}-1)/2$ in (b), by using the lowest 10^9 energy levels starting from the ground state. For comparison we show the Gaussian distribution with the same dispersion (light curved line). $P(W)$ is clearly non-Gaussian.

where T_0 is the period of the shortest classical periodic orbit of (full) geometrical length l_0, and $\overline{N}(E)$ is the total number of levels up to the energy E. Therefore one has

$$\frac{\overline{h}}{T_0} \leqslant E. \tag{73}$$

Now $T_0 = l_0/\sqrt{2E/m}$, m being the mass of the billiard particle, and we find the condition

$$E \geqslant \frac{2\overline{h}^2}{ml_0^2} \tag{74}$$

which at fixed $\overline{h}$ and l_0 is satisfied at all energies E, including the ground state. So, indeed, in two-dimensional billiards the largest energy scales are always in the dynamical saturation (non-universal) regime of $L \geqslant L_{\max}$. The extreme case of classical ergodicity and Gaussian $P(W)$ is stated by the Steiner conjecture.

In our rectangle case we can explain definition (17) also in the following geometrical terms. For our *unfolded* spectral staircase function $N(E)$ we know that its average part goes as E (this is the area inside a quarter of the ellipse of constant E in the plane (m, n)). So, $N_{\text{fluc}}(E) = N(E) - E$. This quantity should then be reduced in terms of the local dispersion, which goes as a square root of the number of objects contributing to the randomness of $N(E)$: but the number of such objects is the number of levels inside a strip of width approximately one and length $\sqrt{E}$ (one quarter of the circumference of the ellipse $E =$ constant). The levels at the grid points (m, n) deep inside the ellipse are well ordered and do not affect the fluctuations of N_{fluc}. So we obtain

$$W(E) = \frac{N(E) - E}{E^{1/4}} \tag{75}$$

which of course agrees with (17), apart from unimportant proportionality constants.

In figure 14 we show the results for our two irrational rectangle billiards, namely for $\alpha = \pi/3$ and $\alpha = (\sqrt{5}-1)/2$. For comparison we plot the Gaussian distribution with the same dispersion as the numerical histograms and this gives a clear and statistically significant evidence for non-Gaussian $P(W)$. In the calculation we have taken into account all the lowest 10^9 levels, starting at the ground state.

4. The two-dimensional torus billiard

The two-dimensional torus billiard is defined by the solutions of the Helmholtz equation on a unit square with periodic boundary conditions, and the energy spectrum is equal to

$$E_{n_1,n_2} = (n_1 - \alpha_1)^2 + (n_2 - \alpha_2)^2 \tag{76}$$

where n_1, n_2 are any integer numbers $0, \pm 1, \pm 2, \ldots$, while α_1 and α_2 are the phases and they are real numbers on the interval $[0, 1)$. They can be generated either by the prescribed change in the phase upon traversing a circuit around the torus, or, for instance, by switching on the magnetic flux. The details of the physical origin of equation (76) are not important here and will not be discussed further.

The Weyl formula for the two-dimensional torus billiard is, according to (20), just

$$\overline{N}(E) = \text{constant} \times E \tag{77}$$

because there is no boundary at all ($\mathcal{L}, \mathcal{K} = 0$). The unfolded energy reads

$$E^r_{n_1,n_2} = \pi((n_1 - \alpha_1)^2 + (n_2 - \alpha_2)^2). \tag{78}$$

This is correct because the mean density of grid points in the (n_1, n_2) plane is one, and thus inside a circle of radius $((n_1 - \alpha_1)^2 + (n_2 - \alpha_2)^2)^{1/2}$ we find on average exactly $E^r_{n_1,n_2}$ grid points.

We shall now analyse the statistical properties of this energy spectrum. To start with we choose some irrational values for the phase parameters, namely $\alpha_1 = 1/e$ and $\alpha_2 = 1/\pi$. In figure 15 we show, in analogy with the irrational rectangle of figure 1, the level spacing distributions $P(S)$, demonstrating the trend towards the Poissonian law $P(S) = \exp(-S)$. The width of the bins here is fixed and equal to $\Delta S = 0.001$. However, if we fix the number of objects in one bin, approximately equal to $N_b \approx 10\,000$, keeping it fixed at all energies, we observe precisely the same behaviour as in figure 3 for the irrational rectangle. As shown in figure 16 the fluctuations are much bigger than statistically expected (relative size $\approx 1/\sqrt{N_b} \approx 0.01$). The phenomenon is again due to the closeness to some rational parameter values where the game of natural numbers reappears.

Indeed choosing some rational values for the phases $\alpha_i = q_i/p_i$, where $i = 1, 2$ and each pair q_i, p_i has no common divisor, we calculate the unfolded energy (78) as

$$E = \pi \left[\frac{p_1 p_2 (n_1^2 + n_2^2) - 2(q_1 p_2 n_1 + q_2 p_1 n_2)}{p_1 p_2} + \left(\frac{q_1}{p_1}\right)^2 + \left(\frac{q_2}{p_2}\right)^2 \right] \tag{79}$$

which, disregarding the simple additive constant, leads to the level spacings which are only integer multiples of the quantity $X_t = \frac{\pi}{p_1 p_2}$. This again suggests the discrete Poissonian model, like in the rectangle billiard of section 3.3, so

$$P_{X_t}(n) = (1 - \exp(-X_t)) \exp(-n X_t). \tag{80}$$

Similarly to as in the rectangle billiard, we could show that the model does not apply to the rational tori (figure 17). The delta spikes at $S \neq 0$ decrease as $1/\sqrt{\ln E}$ (figure 18), although we are not yet far enough in the asymptotic region of sufficiently large $\overline{N}$ to see that the constant B_2 is zero, as we anticipate, but the shape is roughly preserved, i.e. the relative heights of the delta peaks remain approximately constant (figure 19).

The next question is: What happens to the delta spikes when we distort the torus a little away from the rational one (α_1^r, α_2^r), by $(\delta\alpha_1, \delta\alpha_2)$? The delta peaks broaden in a similar

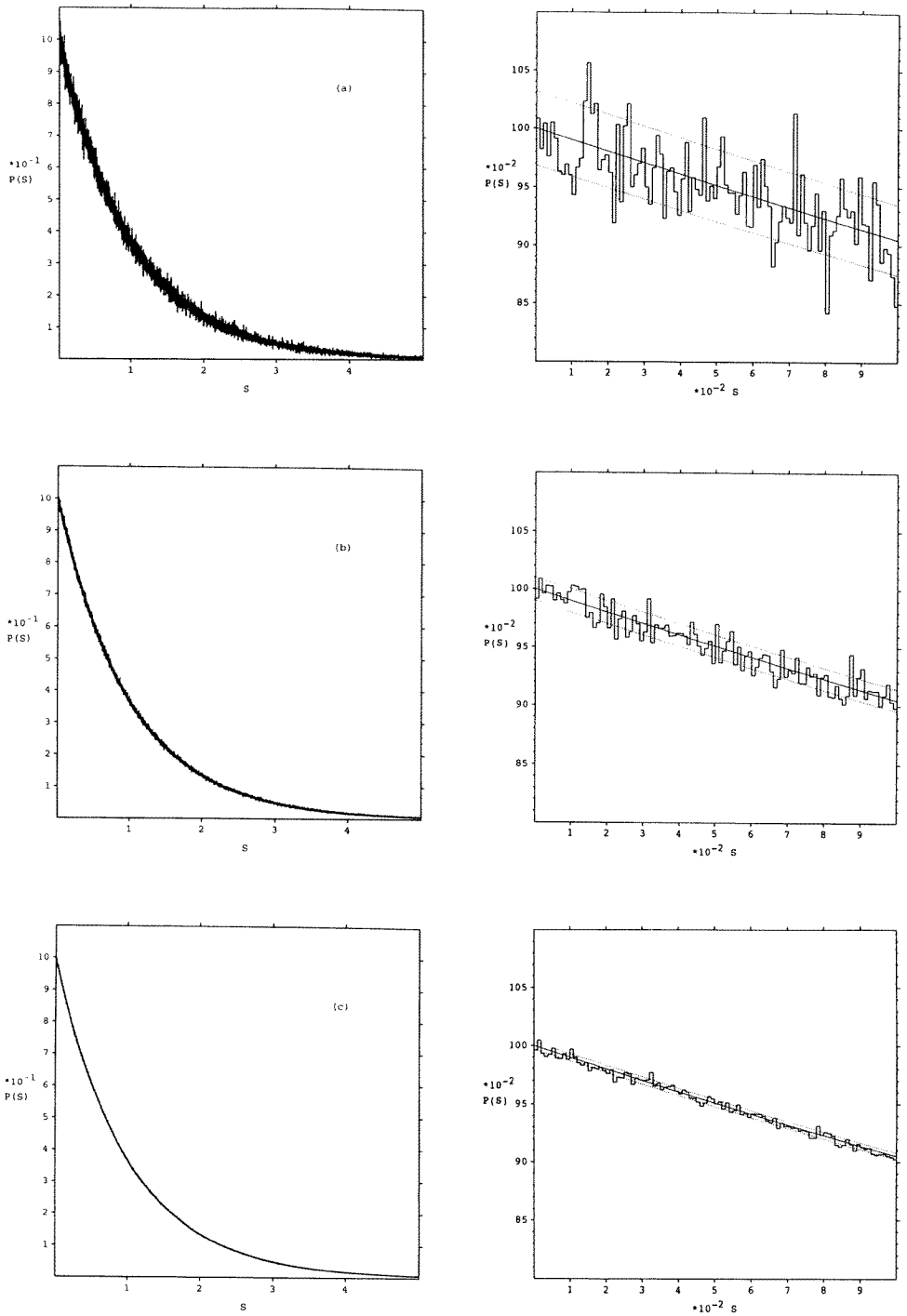

Figure 15. $P(S)$ for the irrational torus $\alpha_1 = 1/e$ and $\alpha_2 = 1/\pi$, in three different energy windows $\mathcal{O}_1, \mathcal{O}_2$ and $\mathcal{O}_3$, as defined in section 3.1, in (a), (b) and (c), respectively. The bin size is fixed and equal to $\Delta S = 0.001$. In each case in the right picture we show enlarged part near $S = 0$, together with the expected $\pm\sigma$ error (dotted), and the theoretical Poissonian curve (full curve).

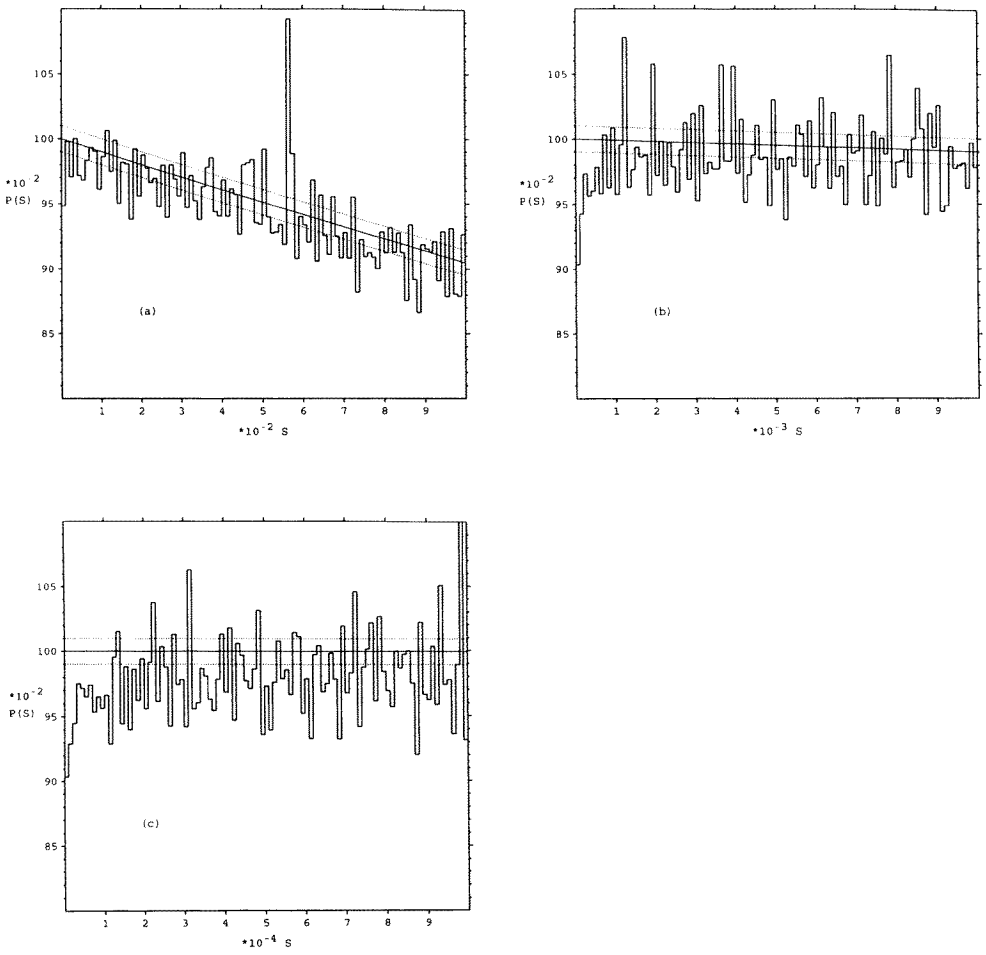

Figure 16. $P(S)$ for the irrational torus $\alpha_1 = 1/e$ and $\alpha_2 = 1/\pi$, for the 10^7, 10^8 and 10^9 lowest energy levels, in (a), (b) and (c), respectively. The bin size is changing with the energy (window) in such a way that the number of objects per bin N_b is approximately constant and equal to $N_b = 10\,000$. The observed fluctuations are clearly much bigger than the statistically expected ones, indicated by the $\pm\sigma$ dispersion band (dotted), while the mean behaviour is in agreement with the Poissonian curve $P(S) = \exp(-S)$ (light full curve).

way to in the rectangle. In fact, it is quite easy to show that one obtains a similar formula for the distribution of the energy shifts δE as for the rectangle, equation (43),

$$\frac{\mathrm{d}w}{\mathrm{d}\delta E} = \frac{1}{\pi}\frac{1}{\sqrt{\Gamma_t^2 - (\delta E)^2}} \qquad \Gamma_t = 2|\delta\alpha|\sqrt{\pi E} \tag{81}$$

except that $\Gamma_t \propto \sqrt{E}$ rather than $\Gamma \propto E$. Here we have denoted by $|\delta\alpha|$ the length of the deformation vector $(\delta\alpha_1, \delta\alpha_2)$. Using this information, and similar reasoning as in section 3.4, we arrive at equations (47) and (48), the only difference being the definition of Γ, which in this case must be equal to Γ_t, defined in the above equation. We have tested this distribution against the data and a similarly good agreement was found as in figure 9, therefore we do not show the results. A similar analysis to in section 3.4, taking into account the higher multiplets, etc, can be performed with the final result exactly as

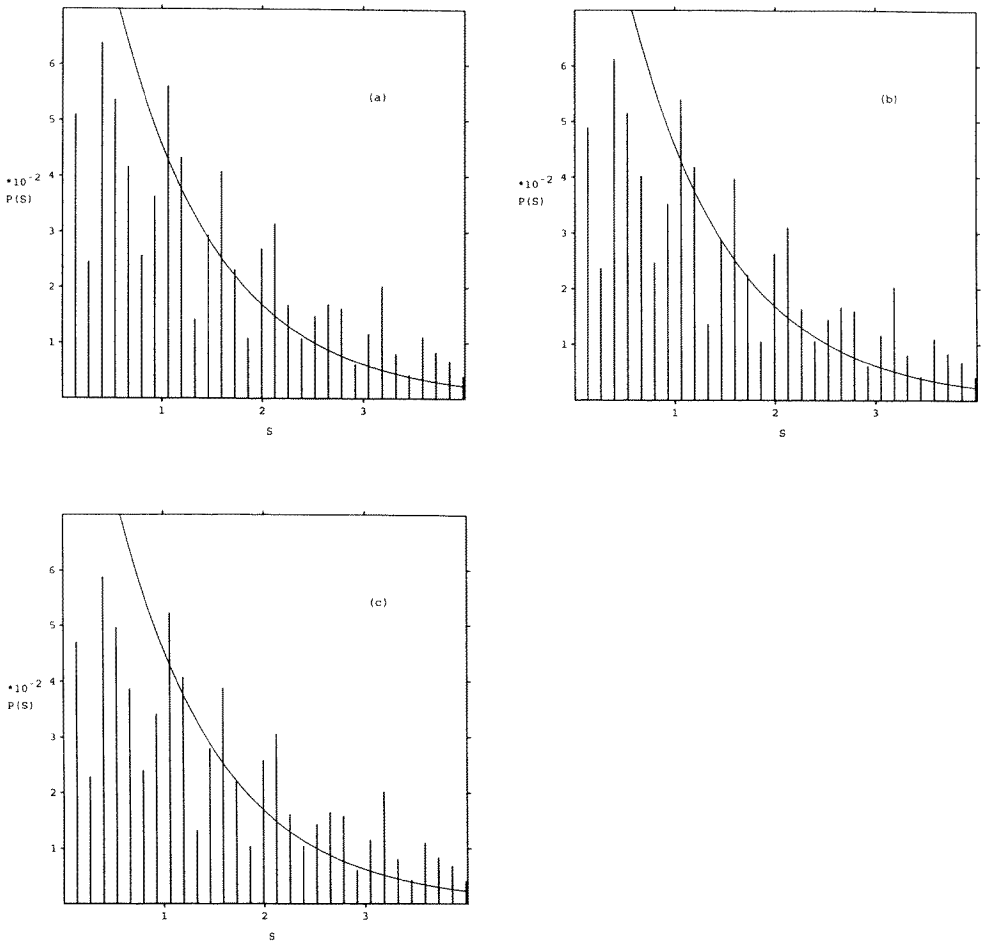

Figure 17. $P(S)$ for the rational torus with $\alpha_1 = \frac{1}{5}$ and $\alpha_2 = \frac{1}{7}$, for the energy windows $\mathcal{O}_1$ - $\mathcal{O}_3$ in (*a–c*), respectively, in comparison with the Poissonian model (80) (full curve). Obviously, the model does not apply.

equation (58), except that instead of Γ we have to use Γ_t, of course. It is clear that the anomalous fluctuations in $P(S)$ of figure 16 are precisely due to the closeness of some rational torus to the irrational one, in excellent analogy with the rectangle billiards. We have also confirmed (but do not show the results) that the $\Delta(L)$ statistics and $E(k, L)$ statistics behave in rational torus in precise analogy with the rational rectangle billiard.

In figure 20 we show the results for the delta statistics for the irrational torus. Up to the saturation regime $L \leqslant L_{\max}$ the agreement with the Poissonian law $L/15$ is excellent. The saturation occurs at a value approximately twice greater than L, because on the torus the shortest classical periodic orbit is twice as short as in the rectangle. In figure 21 we plot the $E(k, L)$ statistics. The interpretation of the results is just the same as in the rectangle billiard of section 3.6.

Finally we analyse the reduced mode number fluctuations, using definition (75). Bleher *et al* (1993) have shown rigorously that the limiting distribution $P(W)$ does exist, and that it has the non-Gaussian tails $P(W) \propto \exp(-W^4)$. Their predictions are tested in figure 22. To

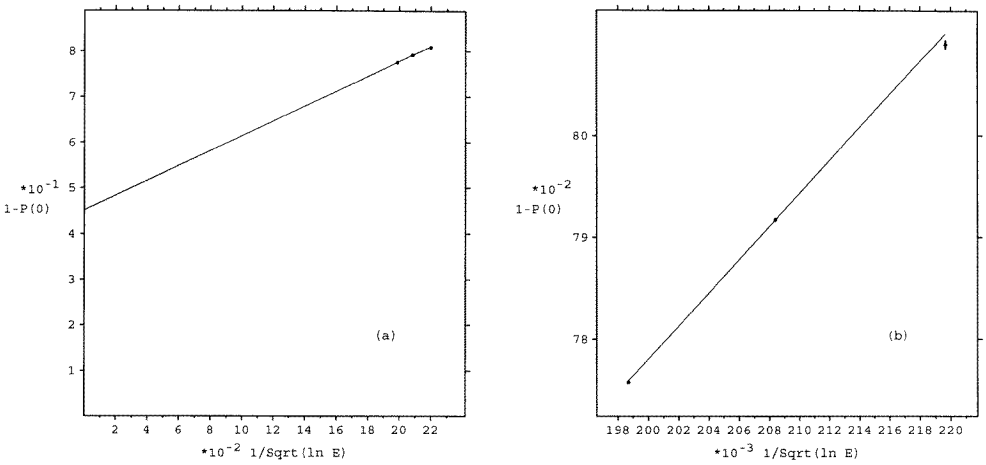

Figure 18. We plot $1 - P_{X_t}(0)$ for the rational torus with $\alpha_1 = \frac{1}{5}$ and $\alpha_2 = \frac{1}{7}$, versus $1/\sqrt{\ln E}$, to test the relationship (34), whose validity is herewith confirmed. In (*b*) we show the enlarged region where the data lie. The value of the extrapolated constant B_2 is not yet zero, probably because we are not yet far enough in the asymptotic region $\overline{N} \to \infty$. $B_2 \to 0$ implies $P_X(0) \to 1$.

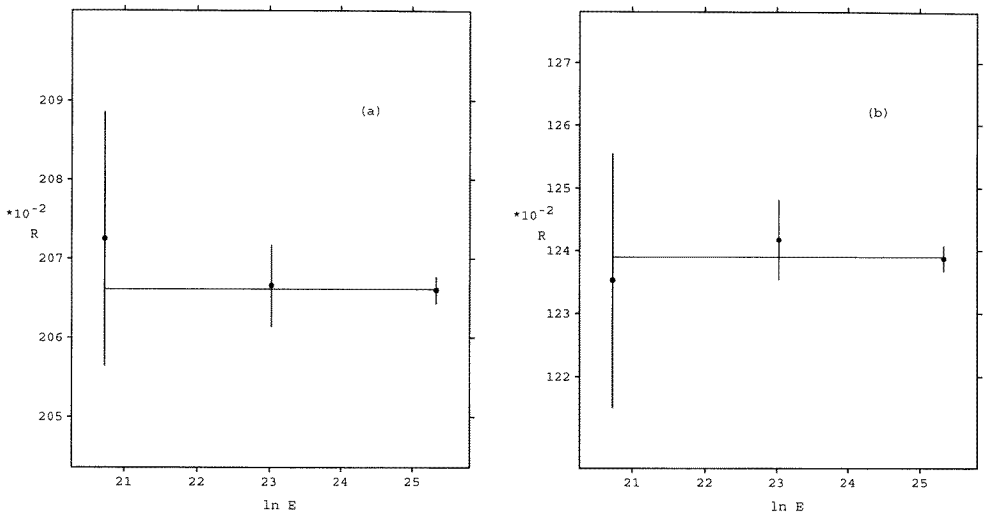

Figure 19. The rational torus with $\alpha_1 = \frac{1}{5}$ and $\alpha_2 = \frac{1}{7}$: We plot the ratios $P_{X_t}(1)/P_{X_t}(2)$ (*a*) and $P_{X_t}(28)/P_{X_t}(29)$ (*b*) versus $\ln E$, showing that the shape of the distribution (80) is approximately preserved as energy increases.

obtain an accurate and statistically reliable confirmation we would have to go substantially higher in energy than 10^9, in order to increase appreciably the number of objects in the tail of $P(W)$.

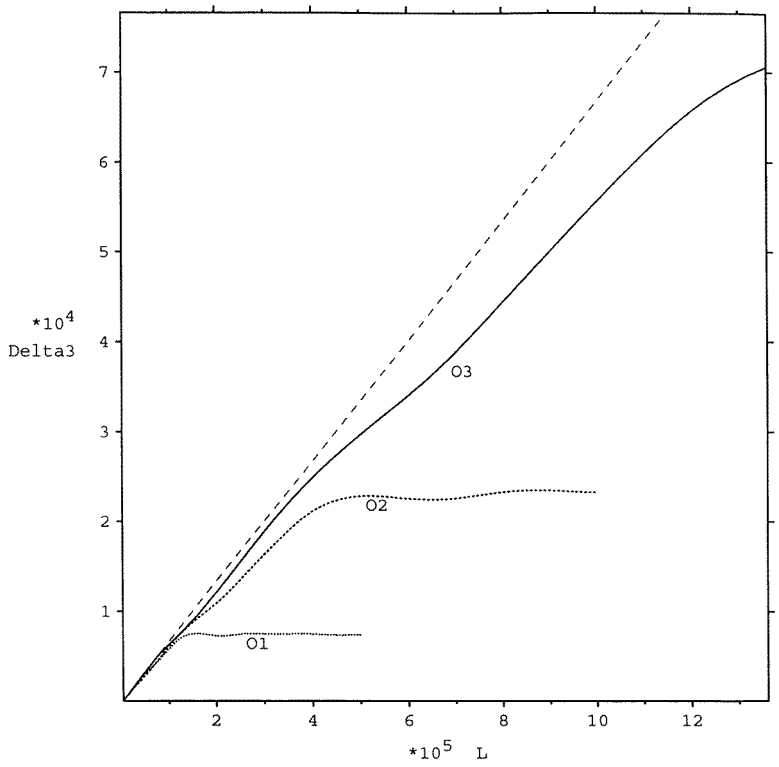

Figure 20. $\Delta(L)$ statistics for the irrational torus with $\alpha_1 = 1/e$ and $\alpha_2 = 1/\pi$, for the three energy windows $\mathcal{O}_1, \mathcal{O}_2$ and $\mathcal{O}_3$, as defined in section 3.1.

5. The circle billiard

As the third model system we have chosen the unit circle billiard. We shall look at the solutions of the Helmholtz equation (19) with Dirichlet boundary conditions. The eigenfunctions are (in polar coordinates r and ϕ)

$$\psi_{\nu,s}(r,\phi) = J_\nu(\xi_{\nu,s} r)\{\cos(\nu\phi), \sin(\nu\phi)\} \tag{82}$$

where J_ν is the Bessel function (of the first kind) of νth order and $\xi_{\nu,s}$ is its sth zero. ν is the absolute value of the angular momentum (quantum number). (Of course, $J_\nu(x) = (-1)^\nu J_{-\nu}(x) = J_{|\nu|}(x)$, and instead of cos/sin functions we could use $\exp(\pm i\nu\phi)$.) The energy spectrum is

$$E = \xi_{\nu,s}^2 \tag{83}$$

and is doubly degenerate for all ν, except for $\nu = 0$. To remove the degeneracy we consider the desymmetrized billiard, namely the semicircle billiard, whose eigenstates are precisely the odd eigenstates (with respect to the reflection across the line $\phi = 0$) of the full circle billiard. Thus, we consider only the eigenstates whose angular part is described by $\sin(\nu\phi)$, and therefore $\nu = 1, 2, \ldots$, and $s = 1, 2, \ldots$. The Weyl formula (20) obtains the form

$$\overline{N}(E) = \frac{1}{8}E - \frac{2+\pi}{4\pi}\sqrt{E} + \frac{1}{8}. \tag{84}$$

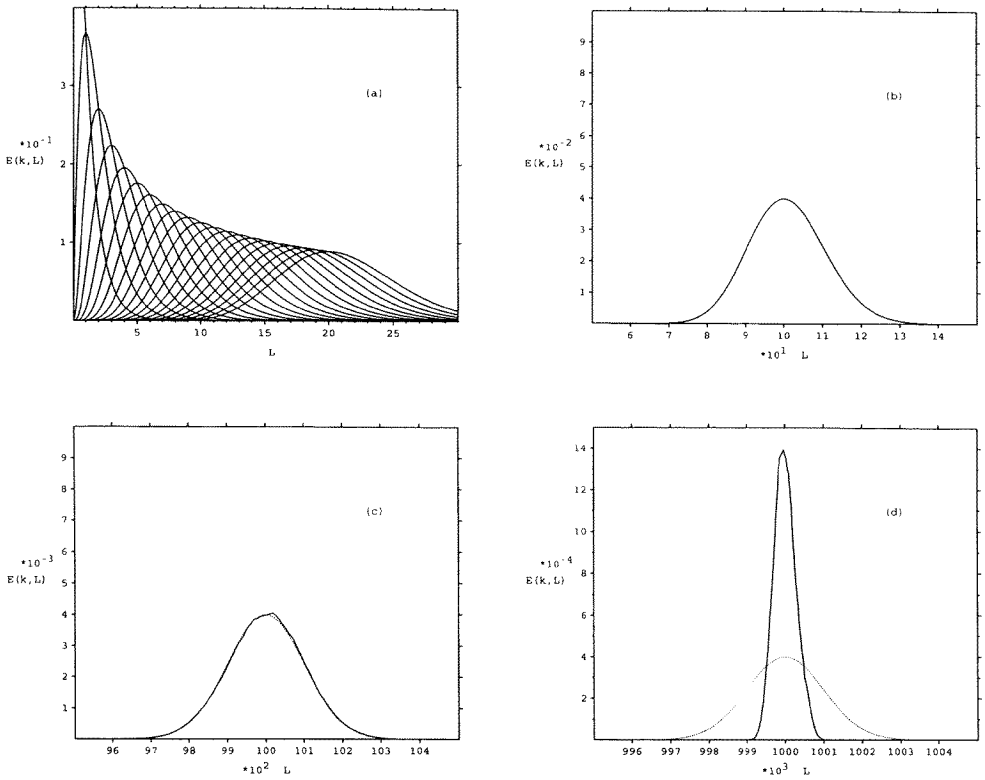

Figure 21. $E(k, L)$ statistics for the irrational torus with $\alpha_1 = 1/e$ and $\alpha_2 = 1/\pi$, for the energy window $\mathcal{O}_3$. In (a) $0 \leqslant k \leqslant 20$, in ($b$) $k = 10^2$, in (c) $k = 10^4$, and in (d) $k = 10^6$. The agreement is excellent up to $k \approx L \approx 10^4$.

The constant $\mathcal{K}$ stems from the contribution $\frac{1}{2} \times \frac{1}{6}$ due to the curvature and $2 \times \frac{1}{48}$ due to two right angles.

We have calculated 1.5×10^7 energy levels for the unit semicircle billiard. In doing so we have carefully checked the numerical routines to ensure that no levels were missed, also by using the Weyl formula (84).

In figure 23 we show $P(S)$ for the semicircle billiard. The general observation is that there is a clear convergence of data towards the Poissonian behaviour, with the fluctuations being of the order as statistically expected. The only unexpected feature are the quite big spikes at integer and half-integer values of S, clearly visible in figure 23(a). It can be shown by the analysis of the asymptotical properties of the zeros of the Bessel functions that such enhanced fluctuations must occur. Due to the lack of space we omit the presentation of this analysis.

As for the long-range correlations for the semicircle we can reconfirm the goodness of the Poissonian model, as manifested in figure 24 for the delta statistics $\Delta(L)$, for scales $L \leqslant L_{\max} \propto \sqrt{E}$, where $E = 1.5 \times 10^7$ and $L_{\max}$ is equal to ≈ 3000.

In figure 25 the $E(k, L)$ statistics for the semicircle is also seen to follow the Poissonian law up to the saturation scale $k_{\max} \approx L_{\max}$. For $0 \leqslant k \leqslant 20$ we see the almost perfect agreement with Poissonian value (12), whilst at $L \approx k \approx 100$ we detect the first notable deviations which articulate at larger k and L in the narrowing of the curves, due to the level clustering.

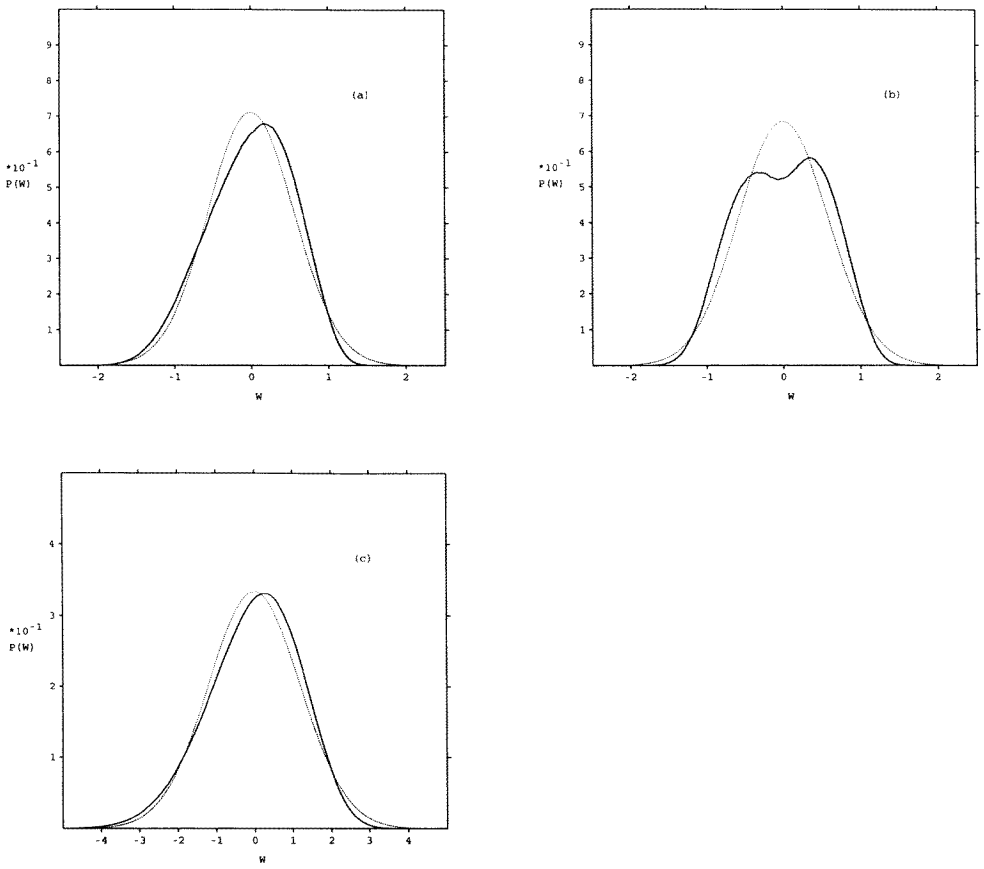

Figure 22. We show the reduced mode number distribution $P(W)$ for the tori: $\alpha = (0.465\,8, 0.018\,14)$ in (a), $\alpha = (0.343\,7, 0.430\,4)$ in (b) and $\alpha = 0$ in (c), as chosen in (Bleher *et al* 1993). In each case we have used 10^9 levels from ground state upwards. For comparison we show the Gaussian distribution with the same dispersion (light dotted). The behaviour of $P(W)$ is obviously not Gaussian, and it seems to decay faster than $\exp(-W^2)$, qualitatively in agreement with (Bleher *et al* 1993), namely $\propto \exp(-W^4)$.

Finally we define the reduced mode number $W(x)$ as in the general equation (17), and specifically for the billiards in equation (75), and study its distribution $P(W)$, using 1.5×10^7 energy levels for the unit semicircle. The result is shown in figure 26, clearly exhibiting deviations from the Gaussian distribution of the same dispersion.

6. Conclusions and discussion

The primary conclusion of this work is that the Poissonian statistical model, defined in section 2, is in fact an excellent approximation for almost all classically integrable systems. By almost all we mean the generic members of the class of integrable systems, the set of exceptions having a small or even vanishing measure in the set. In the rectangle and torus billiards these exceptions arise whenever the billiard is a rational billiard, in which case, for example the level spacing distribution is not a smooth one, but a sum of delta functions positioned at only the integer multiple values of certain basic quantity X. In these rational

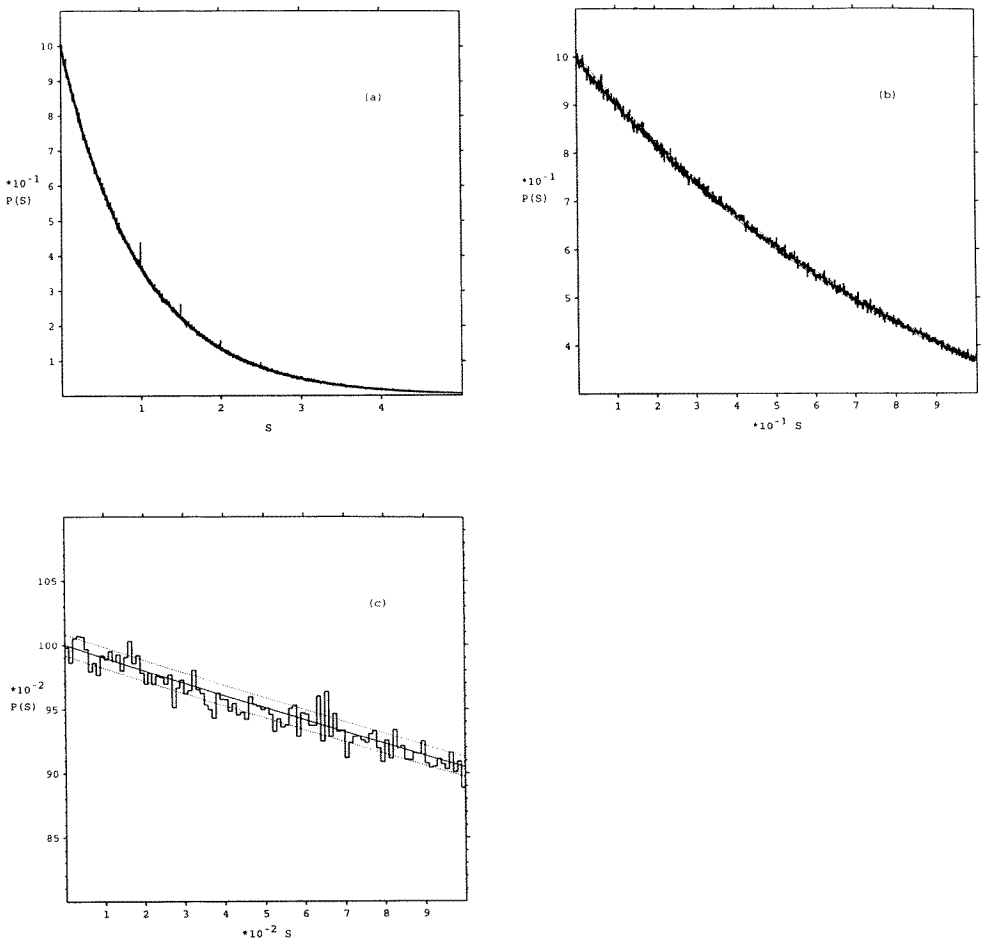

Figure 23. $P(S)$ for the unit semicircle billiard: The bin size is $\Delta S = 0.001$, and we have used 1.5×10^7 energy levels, starting from the ground state. The agreement with Poissonian statistics (light full curve) is excellent, including the size of fluctuations being within the $\pm\sigma$ error band (dotted). The small spikes at integer and half-integer S are explained in the text.

cases even the discrete Poissonian model does not apply: In fact, we even find that all the delta spikes go to zero as $\propto 1/\sqrt{\ln(E)}$, with energy E, so that in the asymptotical $P(S)$ only the zero S delta spike survives and we have $P(S) = \delta(S)$. We have explained the details of such anomalous behaviour, and also presented the theory of what happens if we slightly deform the billiard away from its rational shape. The delta spikes broaden, and have a highly non-trivial distribution, described by the theoretical level spacing shift distribution (58) of section 3.4, which agrees well with the numerical data for the rectangle as demonstrated in figures 7 and 8. Of course, the rational numbers are dense in the set of real numbers, and so every irrational billiard is arbitrarily close to a given rational number q/p of sufficiently high order, with large $q \approx p \gg 1$. Therefore for sufficiently small energies we always see the influence of nearby rational billiards, manifesting itself for example in the anomalous fluctuations in the level spacing distribution $P(S)$ as discovered by Casati *et al* (1985). We have shown, that for the irrational billiards, at sufficiently high energies, in order to escape

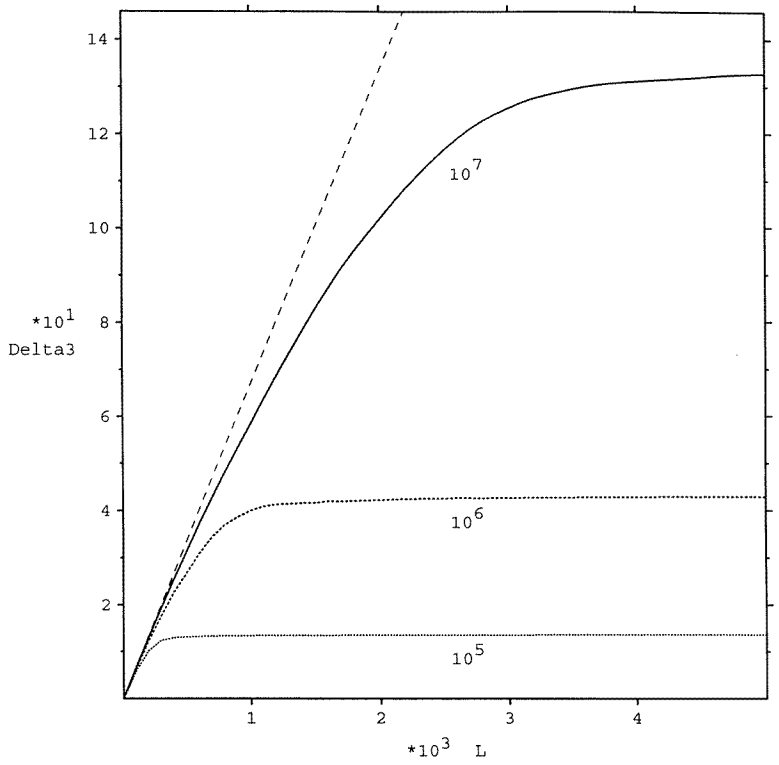

Figure 24. $\Delta(L)$ statistics for the unit semicircle billiard for the first 10^5, 10^6 and 10^7 energy levels (from bottom to top): the agreement with the Poissonian value $L/15$ is very good up to the saturation scale $L_{\max} \propto \sqrt{E}$. The saturation value also scales as $\Delta_\infty \propto \sqrt{E}$.

the influence of the rational billiards, we observe the Poissonian statistics in almost perfect agreement with theory in all $E(k, L)$ statistics, and in particular also in $P(S)$, if the bin size ΔS is kept fixed and not changing with energy. This holds true, however, only at energy ranges up to $L \leqslant L_{\max} \propto \sqrt{E}$, because at $L \geqslant L_{\max}$ we find the saturation phenomena in absolute agreement with the dynamical theory of Berry (1985), which in our work is brilliantly confirmed.

We have also pointed out that in considering the reduced mode number (W) fluctuations and their distribution $P(W)$ we are in fact looking at statistical measures at all scales. It is then argued that in doing so we are always in the saturation regime $L \gg L_{\max}$ and thus $P(W)$ can just be anything, in particular non-Gaussian. A truly Poissonian process $W(x)$ would imply a Gaussian $P(W)$, which is not observed just because of the dynamical saturation regime at such largest energy scales. The non-trivial statement is then the Steiner conjecture (1994) saying that only in the extreme of the classically fully chaotic systems $P(W)$ becomes a Gaussian distribution, with unit dispersion, and so the most random one among all the possible ones. Thus, the conclusion is that the classically chaotic systems indeed have the most random spectra.

Our findings have also been illustrated in cases of the torus billiard and circle billiard, confirming all the aspects given above. In circle, the approach to the Poissonian statistics is the fastest, just because it is far away from non-generic (rational) billiards.

We must comment on two related papers. One is by Casati *et al* (1984), where the

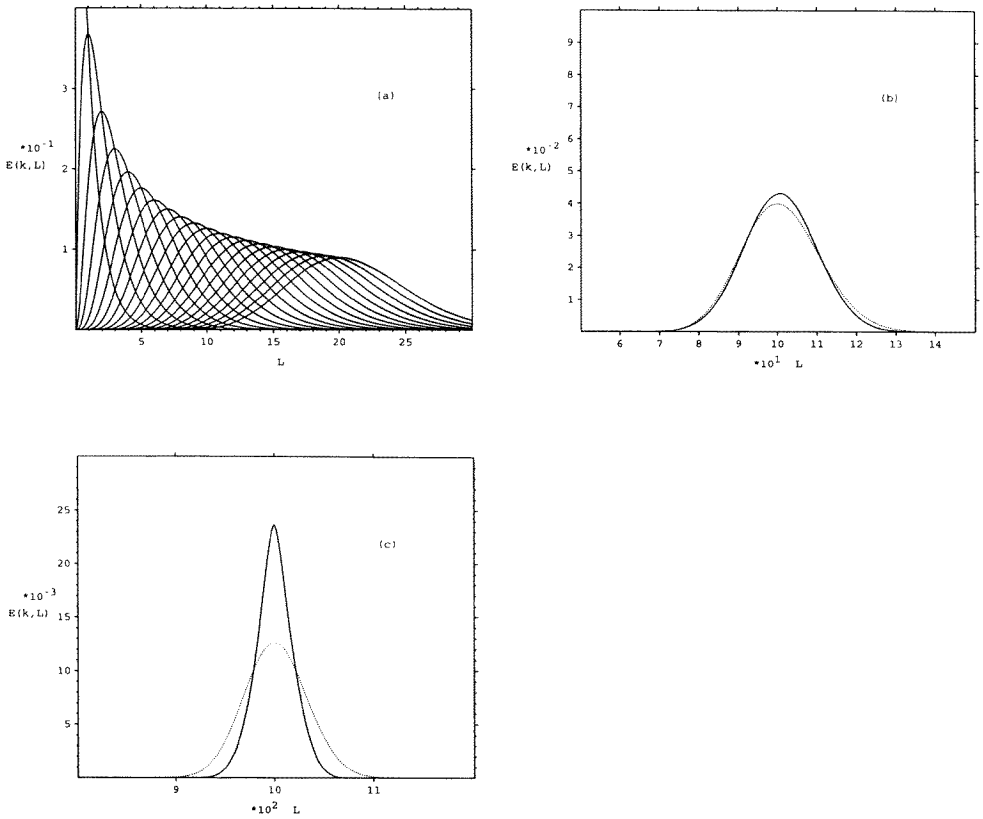

Figure 25. $E(k, L)$ statistics for the unit semicircle billiard for the lowest 1.5×10^7 energy levels. In (*a*) $0 \leqslant k \leqslant 20$, (*b*) $k \approx 100$ and (*c*) $k \approx 1000$. The agreement is good up to $k \approx L \approx 10^2$.

authors show that integrable systems have (unfolded) energy spectra whose algorithmic complexity in the sense of Kolmogorov is zero, which again should imply that the spectra are not random and therefore should not be Poissonian. Their analysis is particularly careful for the case of rectangle billiards. This is in contrast to the case of random matrix theories where the spectrum of a matrix drawn from one of the ensembles (GOE, GUE, GSE), according to Casati *et al* (1984), has positive algorithmic complexity, in agreement with the notion of randomness of such spectra, especially in view of the Bohigas conjecture, where such random models are supposed to apply. It is our opinion that the rigorous meaning and the relationship between the Poissonian behaviour and zero algorithmic complexity must still be assessed and clearly understood. Quite generally, the meaning of algorithmic complexity and its relation to the concept of randomness is likewise still open for the discussion. One possible answer to the paradox might be in realizing that in each specific dynamical system at fixed value of $\hbar$ we always have saturation regime at certain $L \geqslant L_{\max}$, affecting the algorithmic complexity—which is in fact defined only in the limit $L \to \infty$—rendering it zero, perhaps, whilst in random matrices (of infinite dimension) there are no saturation effects.

The second paper is a recent preprint by Marklof (1998), where he proves rigorously that generically the rectangle billiards do not follow the Berry–Tabor conjecture (1977),

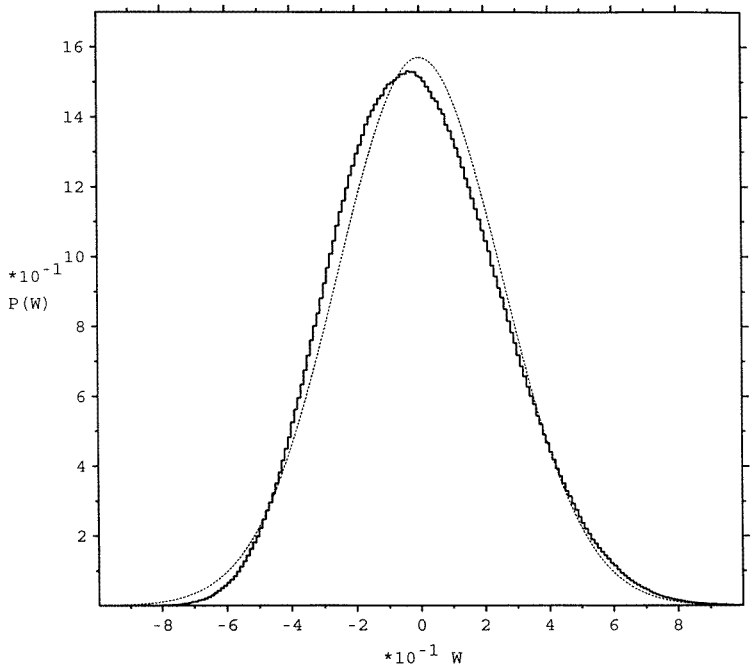

Figure 26. The reduced mode number distribution $P(W)$ for the semicircle for the lowest 1.5×10^7 energy levels (heavy curve), compared with the Gaussian distribution with the same dispersion (light curve). The deviation from the Gaussian is definitely statistically reliable, but is theoretically unknown.

except for local (= short-range) statistics, where the behaviour is indeed Poissonian, thereby confirming the results by Casati *et al* (1984). This statement refers to the typical cases in the parameter space, so it refers to a whole ensemble of systems. However, for individual dynamical systems nothing has been proven so far. It is clear that in an individual system there will always be saturation effects, and therefore rigorously the statistics can never be globally Poissonian at any fixed $\overline{h}$ or finite energy. However, it converges to the Poissonian at larger and larger energy ranges when $\overline{h} \to 0$ or when the energy (the number of levels) goes to infinity, in such a way that we always have $L \ll L_{\max}$.

We may conclude with the bold statement that we almost fully understand the classically integrable systems. They have Poissonian statistics, in the semiclassical limit, at energy ranges L up to the upper scale $L \leqslant L_{\max}(E)$ as a function of the unfolded energy E. The vicinity of a rational system might become more and more visible even at higher energies if we are closer to some rational system, but ultimately we see the approach to the Poissonian behaviour.

There is, however, still a lot of work to be done, especially in the rigorous sense. We want to know more details in the rational cases, we want to understand the limiting $P(W)$ in different systems, along with the important results of Bleher *et al* (1993). On the practical side, the understanding of the classically integrable class of quantal systems in terms of the Poissonian statistics is sufficient to construct the theories for the generic systems, having assumed that we understand the classically chaotic quantal universality classes. A recent account of these topics was offered in Robnik and Prosen (1997) and Robnik (1997).

Acknowledgments

This work was supported by the Ministry of Science and Technology of the Republic of Slovenia and by the Rector's Fund of the University of Maribor.

References

Andreev A V, Agam O, Simons B D and Altshuler B L 1996 *Phys. Rev. Lett.* **76** 3947
Aurich R, Bäcker A and Steiner F 1997 *Int. J. Mod. Phys.* **11** 805
Aurich R, Bolte J and Steiner F 1994 *Phys. Rev. Lett.* **73** 1356
Berry M V 1985 *Proc. R. Soc.* A **400** 229
Berry M V and Robnik M 1984 *J. Phys. A: Math. Gen.* **17** 2413
——1986 *J. Phys. A: Math. Gen.* **19** 669
Berry M V and Tabor M 1977 *Proc. R. Soc.* A **156** 375
Bleher P M, Zheming C, Dyson F J and Lebowitz J L 1993 *Commun. Math. Phys.* **154** 433
Bohigas O 1991 *Chaos and Quantum Physics* ed M-J Giannoni *et al* (Amsterdam: North-Holland) pp 89–199
Bohigas O, Giannoni M-J and Schmit C 1984 *Phys. Rev. Lett.* **52** 1
Casati G, Chirikov B V and Guarneri I 1985 *Phys. Rev. Lett.* **54** 1350
Casati G, Guarneri I and Valz-Gris F 1984 *Phys. Rev.* A **30** 1586
Connors R D and Keating J P 1997 *J. Phys. A: Math. Gen.* **30** 1817
Feingold M 1985 *Phys. Rev. Lett.* **55** 2626
Gradshteyn I S and Ryzhik I M 1994 *Tables of Integrals, Series and Products* (Boston, MA: Academic) p 290
Guhr T, Müller-Groeling A and Weidenmüller H A 1997 *Random Matrix Theories in Quantum Physics: Common Concepts* MPI *Preprint* H V27 MPIfK Heidelberg (cond-mat/9707301, 29 July 1997)
Haake F 1992 *Quantum Signatures of Chaos* (Berlin: Springer)
Hardy G H and Wright E M 1983 *An Introduction to the Theory of Numbers* (Oxford: Oxford University Press)
Keating J and Bogomolny E 1996 *Phys. Rev. Lett.* **77** 1472
Keating J P and Robbins J M 1997 *J. Phys. A: Math. Gen.* **30** L177
Landau E 1908 *Arch. Math. Phys.* II **13** 305
Leyvraz F, Schmit C and Seligman T H 1997 *J. Phys. A: Math. Gen.* **29** L575
Markloff J 1998 *Spectral Form Factors in Rectangle Billiards Preprint* (Orsay: Institut de Physique Nucléaire) (j.marklof@bristol.ac.uk)
Mehta M L 1991 *Random Matrices* (London: Academic)
Prosen T and Robnik M 1993a *J. Phys. A: Math. Gen.* **26** L37
——1993b *J. Phys. A: Math. Gen.* **26** 2371
——1994a *J. Phys. A: Math. Gen.* **27** L459
——1994b *J. Phys. A: Math. Gen.* **27** 8059
Robnik M 1986 *Lect. Notes Phys.* **263** 120
Robnik M 1997 *Open Systems and Information Dynamics* **4** 211–40
Robnik M and Berry M V 1986 *J. Phys. A: Math. Gen.* **19** 669
Robnik M and Prosen T 1997 *J. Phys. A: Math. Gen.* **30** 8787
Robnik M and Salasnich L 1997a *J. Phys. A: Math. Gen.* **30** 1711
——1997b *J. Phys. A: Math. Gen.* **30** 1719
Seligman T H and Verbaarschot J J 1986 *Phys. Rev. Lett.* **56** 2767
Shnirelman A I 1993 *KAM Theory and Semiclassical Approximations to Eigenfunctions* ed V F Lazutkin (Berlin: Springer) (addendum)
Steiner F 1994 *Schlaglichter der Forschung. Zum 75. Jahrestag der Universität Hamburg 1994* ed R Ansorge (Hamburg: Dietrich Reimer) pp 543–64
Weidenmüller H A 1997 Private communication